Lawrence Berkeley National Laboratory

Title
Optics of High-Energy Beams

Permalink
https://escholarship.org/uc/item/5f14306q

Author
Chamberlain, Owen

Publication Date
1960-05-01

UNIVERSITY OF CALIFORNIA

Ernest O. Lawrence

Radiation Laboratory

BERKELEY, CALIFORNIA

OPTICS OF HIGH-ENERGY BEAMS[1,2]

By Owen Chamberlain

Physics Department University of California, Berkeley, California

INTRODUCTION

Many of the experiments now being conducted on high-energy accelerators require the use of beams of charged secondary particles. It is worth while at this time to attempt to summarize information about some of the most useful methods of setting up such beams.

We are not concerned here with the primary beam of the accelerator. Rather, we assume that a target is struck by the primary beam and that it is desired to form a beam from the *secondary* charged particles that emerge from collisions within the target.

The simplest system of forming this beam of secondary particles involves the use of magnetic fields only. In most cases it is desirable to obtain a beam of particles of known magnetic rigidity, or momentum. The bulk of this article is addressed to this problem. Some comments are also made about the use of electric fields in conjunction with magnetic fields. The inclusion of electric fields allows the separation of a beam of known momentum into its various components according to the velocities of the particles, hence according to the masses of the particles. These are referred to as "separated beams."

The curvature K of a charged particle moving in a magnetic field is given by

$$K = (eB)/(pc)$$

where e is the charge in electrostatic units, B is the magnetic induction in gauss, p is the momentum in cgs units, and c is the velocity of light in cm./sec. The curvature K is given in cm.$^{-1}$, and is the reciprocal of the radius of curvature. In the above expression, it has been assumed that the particle moves in a direction perpendicular to the direction of the field B. If the velocity and field are not perpendicular, the curvature vector may be given as

$$K = (dp/ds)/p = (ev \times B)/(pvc)$$

where v is the particle velocity in cm./sec. and ds is an increment of distance along the trajectory of the particle. The curvature is perpendicular to the field B (and by definition perpendicular to the velocity v). The magnitude of the curvature clearly depends upon the component of B perpendicular to v.

In most cases the momentum of beam particles is given in the unit Mev/c. (Momentum in Mev/c is numerically equal to pc in Mev.) If we restrict our attention to particles of single charge (4.8×10^{-10}) esu and measure the momentum in Mev/c, then our expression for the curvature in a magnetic field reduces to

$$K = 3.00 \times 10^{-4} B/p, \qquad B_\rho = [p(\text{in Mev/c})]/[3.00 \times 10^{-4}]$$

ρ being the radius of curvature in field B. This form is the most convenient for our discussion. It resembles closely the well-known form

$$B_\rho = p(\text{in ev/c})/300$$

Nearly all the arrangements in use for forming beams of secondary particles have B field patterns with a plane of symmetry. We therefore restrict

Nearly all the arrangements in use for forming beams of secondary particles have B field patterns with a plane of symmetry. We therefore restrict our attention to systems with such symmetry, and for convenience in explanation we speak as though this plane is always a horizontal plane. With respect to this plane of symmetry, which we call the "central plane," the system should have the following characteristics.

(a) The magnetic field in the central plane is perpendicular to the central plane.

(b) Every north magnetic pole above the central plane is accompanied by a south pole of equal magnitude at the mirror point below the central plane.

(c) To every current element above the plane there is a corresponding current element of equal magnitude whose position and direction are obtained by mirror reflection in the central plane.

(d) A drawing of the magnetic field lines will exhibit reflection symmetry with respect to the central plane; however, the direction of the magnetic field below the plane is opposite to that given by simple reflection.

This symmetry should be obvious in all the systems to be discussed. Of course, we want to make occasional use of further symmetry properties in special cases.

Because of the reflection symmetry assumed, the field in the central plane is perpendicular to the central plane. We choose this upward direction as the z direction, so that we have B_z as the only field component in the central plane. In principle the field is everywhere known once B_z is known throughout the central plane because the conditions

$$\nabla \times B = 0$$

and

$$\nabla \cdot B = 0$$

allow all derivatives of the field components with respect to z to be computed in terms of derivatives of B_z in the central plane. In practice this usually means the field is completely known only fairly close to the central plane, since it is not feasible to obtain such accurate data in the central plane that high-order derivatives can be evaluated with good accuracy.

BASIC COMPONENTS OF PURELY MAGNETIC SYSTEMS

For experiments conducted in connection with magnetic accelerators such as cyclotrons and synchrotrons, the first magnetic component is frequently the field of the accelerator itself. The magnetic field of the accelerator is usually available in the form of a plan view showing contours of equal B_z in the central plane.

For most applications it is essential to perform a momentum analysis in the process of forming a charged-particle beam. This is frequently accomplished by the use of deflecting magnets such as that shown in Figure 1. This magnet has been designed to approximate a uniform field within a rectangular region in the central plane. However, other field distributions are frequently used and can be made by using tapered pole pieces.

For the formation of the most useful beams some focusing properties are essential. Most deflecting magnets have some focusing action, but it is usually too weak to accomplish the desired effect. An important and valuable component is a magnetic lens made of quadrupole magnets. The field pattern of a quadrupole magnet is shown in Figure 2. Quadrupole magnets were introduced in 1952 by Courant, Livingston & Snyder (1) along with the strong-focusing synchrotron. A single quadrupole magnet has a focusing action for motion in one plane (either horizontal or vertical) and a defocusing action in the other plane. However, two or more quadrupole magnets may

...approaches this direction. A simple quadrupole magnet has a focusing action ... in one plane (either horizontal or vertical) and a defocusing action ... the other plane. However, two or more quadrupole magnets may ... give a net focusing action in both planes and, in fact, to produce a ... lens that closely approximates a simple thin lens of the type used in optics for visible light. Notice that quadrupole magnets, if oriented ... as shown in Figure 2, have the desired symmetry property with respect to a central (horizontal) plane.

DETERMINATION OF A TRAJECTORY IN THE CENTRAL PLANE

In designing a magnet system, one of the first steps is to determine one ... through the system, which may involve the magnetic field of an ... We may call this trajectory the central ray or central orbit. On the basis of a contour map of B in the central plane, it is a simple matter to ... trajectories (orbits) in the central plane for particles of given ... One usually starts from a specified point, which may be the location of a target, and computes an orbit for a particle that leaves the target in a ... specified direction. Alternatively, one may trace the orbit in ... back from a known point toward which the desired ... for example, one may compute backward from an existing ... to determine where a target should be placed.

A trajectory may be determined by numerical integration, perhaps with the help of an electronic computer, with the use of a mechanical orbit plotter such as that described by Rankin (2), or by a graphical method. An example of the graphical tracing of a trajectory is shown in Figure 3, for a hypothetical case. The orbit is approximated piecewise by circular arcs. In the figure the first arc extends from the target center on the contour of 12,000 gauss to the contour of 8000 gauss, being drawn with the radius of curvature appropriate

[footnote] The survey of literature pertaining to this chapter was concluded in May, 1960.
[footnote] Among the abbreviations used in this review is: r.f. (radio frequency).

strong focusing synchrotron. A single quadrupole magnet has a focusing action for motion in one plane (either horizontal or vertical) and a defocusing action for the other plane. However, two or more quadrupole magnets may be used to give a net focusing action in both planes and, in fact, to produce a magnetic lens that closely approximates a simple thin lens of the type used in optics for visible light. Notice that quadrupole magnets, if oriented in the way shown in Figure 2, have the desired symmetry property with respect to a central (horizontal) plane.

Determination of a Trajectory in the Central Plane

In designing a magnet system, one of the first steps is to determine one trajectory through the system, which may involve the magnetic field of an analyzer. We may call this trajectory the central ray or central orbit. On the basis of a contour map of B in the central plane, it is a simple matter to assign trajectories (orbits) in the central plane for particles of given momentum. One usually starts from a specified point, which may be the position of a target, and computes an orbit for a particle that leaves the target in some specified direction. Alternatively, one may trace the orbit in reverse, computing back from a known point toward which the desired particles are aimed; for example, one may compute backward from an existing collimator to determine where a target should be placed.

A trajectory may be determined by numerical integration, perhaps with the help of an electronic computer, with the use of a mechanical orbit plotter such as that described by Rankin (2), or by a graphical method. An example of the graphical tracing of a trajectory is shown in Figure 3, for a hypothetical case. The orbit is approximated piecewise by circular arcs. In the figure the first arc extends from the target center on the contour of 12,000 gauss to the contour of 8000 gauss, being drawn with the radius of curvature appropriate

_____

[1] The survey of literature pertaining to this chapter was concluded in May, 1960.

[2] Among the abbreviations used in this review is: r.f. (radio frequency).

as 10,000 gauss. Through the end-point of the first arc and through the center C 1 of the first arc, the radius line can be extended to the new center C 2, whose position is such as to give a new radius appropriate to the average field over the next circular arc, in this example 6000 gauss. The second arc can then be drawn about C 2 as center and extending to the 4000 gauss contour. The third arc is drawn similarly, extending to the 2000 gauss contour. Finally, a straight line (at right angles to the line through the end of the last arc and C 3) is used to carry the orbit into the weak-field region with a deflection at point D to take account of the total field beyond the 2000 gauss contour. The angle of deflection (in radians) at D is $\theta_D = (\int B ds)/(B\rho)$. The position of the point D may be fixed as $s(\int B s ds)/(\int B ds)$. The integrals are carried along the approximate orbit from the end of the last arc. It should be emphasized that the example shown in Figure 3 is done in exceptionally coarse steps to make the diagram clear. In practice, it appears that each arc should cover only about a 20 per cent range of field values if the final orbit is to correspond to the proper momentum to within about 1 per cent. (If the field plot is not drawn to actual size, the radii of curvature must obviously be scaled to correspond to the scale of the drawing.)

Clearly, other magnets, such as deflecting magnets, may be treated in the same way to obtain orbits. However, if the deflecting magnets are constructed like that shown in Figure 1, the field contours are very nearly straight lines and it is usually satisfactory to make the simplifying assumption that the region of field is rectangular, being full field within that rectangle and zero outside. The length of the rectangle is the so-called effective length of the field defined by

$$L_{\text{eff}} = \left(\int B ds \right) / B_{\text{max}}$$

Here B_{max} is the maximum field and the integral is to be taken over a straight line through the magnet aperture perpendicular to the entrance edge of the pole face. The effective length usually exceeds the physical length of the iron pole face by about one gap width (being one-half gap width at each end). The advantage of the proposed simplification is that it allows the trajectory within the deflecting magnet to be constructed as one circular arc.

A quadrupole magnet has zero field along its center line so that the central orbit is usually, in the vicinity of the quadrupole, a straight line coincident with the quadrupole axis. The focusing properties are discussed in another section.

FOCUSING PROPERTIES OF MAGNETIC FIELDS

It is usually quite important to know the focusing properties of a magnetic field and to adjust the focusing properties to achieve the desired result. We consider separately the focusing in the horizontal plane and in the vertical plane.

In the horizontal plane, we may first study two orbits that leave the target center in slightly different directions, perhaps tracing the two rays by the graphical method mentioned in connection with Figure 3. An example is shown in Figure 4 of a target within the magnetic field of an accelerator and with one deflection magnet in the system. It is usually assumed that the system is linear enough for two adjacent orbits that interpolation may be used to determine positions and directions of intermediate orbits. Figure 4

is shown in Figure 4 of a target within the magnetic field of an accelerator and with one deflection magnet in the system. It is usually assumed that the system is linear enough for two adjacent orbits that interpolation may be used to determine positions and directions of intermediate orbits. Figure 4 shows the apparent target positions, as viewed from certain points along the beam for particles of the particular momentum for which the orbits have been calculated. The figure shows as dashed lines the straight lines extended backwards to their intersection to determine the apparent target positions.

It is also valuable to know the apparent magnification of the target as viewed through the system. This may be accomplished by tracing an orbit that starts at one edge, rather than the center, of the target. One such orbit is shown as a series of dots in Figure 4. Again dashed lines are used to show straight lines extended backward to determine the size of the apparent target. Usually an unrealistically large target must be assumed so that graphical errors may be minimized.

There is an alternative method for finding the behavior of orbits close to the central orbit. Once a central orbit has been determined graphically, a simple differential equation may be solved numerically to find the focusing properties. The theory given here is a linear theory, adequate providing the orbits under consideration do not deviate too much from the central orbit. Figure 5 illustrates the terminology used here. The deviation (in the central plane) of some orbit from the central orbit is called η and is measured perpendicular to the central orbit. Figure 5 is drawn for a positively charged particle moving in a field directed out of the plane of the figure with η taking a positive value. The differential equation for η as a function of s, the distance along the central orbit, is

$$\frac{d^2\eta}{ds^2} = -\left[\frac{1}{B\rho}\frac{dB_z}{d\eta} + \frac{B_z^2}{(B\rho)^2}\right]\eta$$

Here, B_z is the magnetic flux density along the central orbit, and $dB_z/d\eta$ is the space rate of change of B_z along a line perpendicular to the orbit (and in the direction of positive η as indicated in Fig. 5) evaluated at the central orbit.

The differential equation can be used to determine the same properties for which we have used the construction shown in Figure 4, once a suitable central orbit has been determined. To determine the apparent source positions we would use starting values at the target of perhaps $\eta = 0$, $d\eta/ds \neq 0$. Then, to determine the apparent source sizes we would use as initial values $\eta \neq 0$, $d\eta/ds = 0$. In each case the differential equation would be integrated numerically along the trajectory from the target point. The results would be interpreted as suggested by Figure 4 to determine the (horizontal-plane) apparent target position and size.

The same theory may also be constructed for a deviating orbit of a particle that differs slightly in momentum from the momentum corresponding to the central orbit. There is then an additional term.

$$\frac{d^2\eta}{ds^2} = -\left[\frac{1}{B\rho}\frac{dB_z}{d\eta} + \frac{B_z^2}{(B\rho)^2}\right]\eta + \frac{B_z}{B\rho}\frac{\delta_p}{p}$$

Here $\delta p/p$ is the fractional change in momentum with respect to the central momentum. The equation is, in the author's experience, ascribable to Fermi (3). Here B_z is to be taken as positive if the field is directed out of the plane of the figure. The quantity $B\rho$ is to be given a positive sign for a positively charged particle and a negative sign for a negative particle.

The focusing properties for orbits that deviate vertically from the central orbit can also be handled in a similar way. Because of the zero divergence

form (5). Here B_z is to be taken as positive if the field is directed out of the plane of the figure. The quantity $B\rho$ is to be given a positive sign for a positively charged particle and a negative sign for a negative particle.

The focusing properties for orbits that deviate vertically from the central orbit can also be handled in a similar way. Because of the zero divergence and zero curl of the flux density B the vertical focusing may be related to the same normal derivative $dB_z/d\eta$ that has been used for the horizontal focusing. The differential equation is

$$\frac{d^2\zeta}{ds^2} = -\frac{1}{B\rho}\frac{dB_z}{d\eta}\zeta$$

Here ζ is the vertical displacement of the deviating orbit as measured from the central plane or from the central orbit. Again, the expression is linear in the displacement. The sign conventions are the same as those given above. This differential equation can be used for all cases for which the central orbit lies in the central plane.

For deflecting magnets with uniform field B_0 (or that can be approximated by a region of uniform field), some simple expressions are useful. Vertical focusing occurs only where the central orbit enters or leaves the magnetic field region, and then only when the orbit is other than normal to the boundary line of the field region. The vertical focusing acts like a thin lens at the entrance point and another thin lens at the exit point, the focal length F_v being in either case given by

$$1/F_v = (1/\rho)\tan\theta \quad \text{(entrance or exit of deflecting magnet with uniform field)}$$

where ρ is the radius of curvature in the field, or $(B\rho)/B_0$, and θ is the angle between the central orbit and the normal to the boundary line of the field region. Figure 6 shows θ_1 at entrance and θ_2 at exit, for positive θ_1 and θ_2. For the horizontal focusing it is convenient to measure the object distance p'_H from the entrance boundary and the image distance q'_H from the exit boundary. The expression relating object and image distances is

$$\arctan\left[(\rho/p'_H) + \tan\theta_1\right] + \arctan\left[(\rho/q'_H) + \tan\theta_2\right] = \alpha$$
$$\text{for horizontal focussing, uniform field}$$

for horizontal focusing, uniform field, where α is the bending angle of the central orbit in the magnet. Notice p'_{II} and q'_{II} are measured from entrance and exit points of the effective region of uniform field. Extensive discussions of magnets with uniform field have been given by Cross (4), by Bainbridge (5), and by Buechner (6). Judd (7), and Sternheimer (8) have analyzed instruments involving non-uniform fields.

The methods discussed above should be adequate for almost all magnetic components except quadrupole magnets (or strong-focusing magnets). A typical quadrupole magnet is shown in end view in Figure 7. Figure 8 shows side and top views in cross section, with typical deviating orbits. The central orbit is assumed to lie on the center line. Notice that a single quadrupole is focusing for deviations in one plane and defocusing for deviations in the other plane.

The field within the poles of the quadrupole is intended to conform to the following expressions. We take the x axis to be along the orbit in the forward direction, the z axis to be vertically upward out of the central (horizontal) plane, and the y axis to be fixed to make a right-handed co-ordinate system.

$$B_z = \alpha y$$

$$B_y = \alpha z$$

The simplest treatment of quadrupole focusing involves assuming that the magnetic flux density is given by these expressions throughout the length of the pole pieces and a short distance beyond at each end. The full length over which the field is assumed to be of the given form is then called the effective length l. To fair approximation the effective length is given by

$$l = l_{p+a}$$

where lp is the length of the iron poles and a is the aperture radius shown in Figure 7. The field is then assumed to be zero beyond the region of the effective length. Unfortunately this field, as given, does not satisfy Maxwell's equations because the curl of the field does not vanish near the ends of the quadrupole. Nevertheless, very useful calculations of orbits can be made with this assumed field, neglecting the effects of the fringing field that must inevitably be present.

Within the quadrupole field, the curvature of the orbit that deviates in the y direction from the central orbit along the center line is

$$\frac{\dfrac{d^2 y}{dx^2}}{\left(1 + \left(\dfrac{dy}{dx}\right)^2\right)^{3/2}} = \frac{B_z}{B\rho} = \frac{\alpha y}{B\rho}$$

By assuming $dy/dx \ll 1$ we may justify neglect of the second-order correction in dy/dx and use

$$\frac{d^2 y}{dx^2} = -\frac{\alpha}{B\rho} y = -k^2 y \qquad \text{(focusing plane)}$$

where we have defined $k^2 \equiv \alpha/B\rho$. This set of approximations (and its consequences) is termed the "linear" theory. The resulting linear equation may be solved to give the focal length

$$f = 1/|k \sin (kl)|$$

The principal plane, from which the image distance is to be measured, is located inside the effective quadrupole a distance

$$x_p = [1 - \cos (kl)]/[k \sin (kl)] \cong \frac{l}{2} [1 + (kl)^2/12] \cong l/2;$$

The last approximation is somewhat more crude than necessary.

In the defocusing plane the corresponding expressions are

$$\frac{d^2 z}{dx^2} = \frac{\alpha}{B\rho} z = k^2 z \qquad \text{(defocusing plane)}$$

where $k^2 = \alpha/B\rho$, as before. The focal length is

$$f = -1/[k \sinh (kl)] \qquad \text{(defocusing plane)},$$

and the principal plane is inside the quadrupole a distance

$$x_p = [\cosh (kl) - 1]/[k \sinh (kl)] \qquad \text{(defocusing plane)}$$

where x_p is measured from the effective end of the quadrupole.

This linear theory is extremely useful and is for many purposes adequate. A computationally convenient form of this theory, given by Stork (9), is reproduced here.

We use l to indicate the effective length of a quadrupole. The object distance, measured from the entrance effective end of a quadrupole magnet, is designated p'. The image distance q' is measured from the exit effective end. (The similarity to a simple lens is lost here because the object and image distances are not measured from either the magnet center or principal planes; however, the method presented here is very useful in practice.) The expression for the image distance q' and magnification m are given by

$$q' = [p' \cos (kl) + (1/k) \sin (kl)]/[p'k \sin (kl) - \cos (kl)] \qquad \text{(focusing plane)}$$

$$m = -1/[p'k \sin (kl) - \cos (kl)]$$

in the focusing plane. By expressing lengths in terms of the effective length l of the quadrupole we may simplify further. We use

$$P' = p'/l, \qquad Q' = q'/l, \qquad L = kl$$

Then,

$$Q' = [P' \cos L + (1/L) \sin L]/[P'L \sin L - \cos L]$$

$$m = -1/[P'L \sin L - \cos L] \qquad \text{(focusing plane)}$$

or

$$Q' = [P' + (1/L) \tan L]/[P'L \tan L - 1] \qquad \text{(focusing plane)}$$

The corresponding expressions for reduced image distance (from the effective end of the quadrupole) and magnification m in the defocusing plane are

$$Q' = -[P' + (1/L) \tanh L]/[P'L \tanh L + 1] \qquad \text{(defocusing plane)}$$

$$m = 1/[P'L \sinh L + \cosh L]$$

The relations above are sufficient to describe any quadrupole in first-order theory. For convenience in use, these relations are summarized graphically in figures 9, 10, and 11. Usually the graphs are used to obtain approximate values of L that are appropriate to a given problem, and the final calculations are performed numerically through the use of the algebraic expressions above. (The necessary field measurements can be made with a rotating-coil gaussmeter such as the Rawson Model 720.)

Two or three quadrupoles may frequently be combined to make a lens.

expressions above. (The necessary field measurements can be made with a rotating-coil gaussmeter such as the Rawson Model 720.)

Two or three quadrupoles may frequently be combined to make a lens. Figure 12(a) shows two quadrupoles of equal length (and opposite polarity) assembled to form a "doublet" lens. Figure 12(b) shows what is known as a quadrupole "triplet," each quadrupole being of opposite polarity to the next quadrupole.

Whether a lens should be a doublet or a triplet is a question about which there has been some difference of opinion. Each has advantages and disadvantages. Doublets are less expensive for a given lens strength at a given particle momentum. Doublets have somewhat peculiar focusing properties, in that even if they are adjusted to be without astigmatism they give magnifications in the horizontal and vertical planes. In some problems this is a great advantage for doublets, but it makes them somewhat harder to think about. Triplets, on the other hand, behave rather like a simple thin lens located at the center of the triplet and, therefore, are relatively easy to deal with. Triplets have also the advantage that their focal length (focal length of the combined lens) changes somewhat less rapidly with beam particle momentum. Probably the novice is better off using triplets, but the best design frequently involves using some doublet lenses.

The expressions given above for the image distance q', measured from the effective end of the quadrupole, can very readily be applied twice to give the net result of the two quadrupoles of a doublet lens. The object distance from the effective entrance end of the first quadrupole would be indicated by p'_1. The image distance from the effective exit end of the first quadrupole q'_1 would be related to the object distance p'_2 for the second quadrupole by

$$q'_1 + p'_2 = g$$

where g is the effective gap between quadrupoles as indicated in Figure 12. Usually the two quadrupoles of a doublet are of the same effective length l, so that it is convenient to use the normalized forms in which distances are measured in terms of l. With the definition

$$G = g/l$$

we have, for the plane in which the first quadrupole is focusing and the second is defocusing,

$$Q'_1 = [P'_1 + (1/L_1)\tanh L_1]/[P'_1 L_1 \tanh L_1 - 1]$$

$$m_1 = -1/[P'_1 L_1 \sin L_1 - \cosh L_1]$$

$$P'_2 = G - Q'_1$$

$$Q'_2 = [P'_2 + (1/L_2)\tanh L_2]/[P'_2 L_2 \tanh L_2 + 1]$$

$$m_2 = -1/[P'_2 L_2 \sinh L_2 + \cosh L_2]$$

$$m = m_1 m_2 = -1/([P'_1 L_1 \sin L_1 - \cosh L_1][P'_2 L_2 \sinh L_2 + \cosh L_2])$$

For the other plane (for which the first quadrupole is defocusing) we have

$$Q'_1 = -[P'_1 + (1/L_1)\tanh L_1]/[P'_1 L_1 \tanh L_1 + 1]$$

$$m_1 = 1/[P'_1 L_1 \sinh L_1 + \cosh L_1]$$

$$P'_2 = G - Q'_1$$

$$Q'_2 = [P'_2 + (1/L_2)\tan L_2]/[P'_2 L_2 \tan L_2 - 1]$$

$$m_2 = -1/[P'_2 L_2 \sin L_2 - \cos L_2]$$

$$m = m_1 m_2 = -1/([P'_1 L_1 \sinh L_1 + \cosh L_1][P'_2 L_2 \sin L_2 - \cos L_2])$$

Notice that in the above expressions $L_1 = k_1 l$ is usually different from $L_2 = k_2 l$, corresponding to different magnetizations of the two quadrupoles. Notice also that the same notation is used for the reduced object and image distances, such as Q'_1, whether they refer to focal properties in the horizontal or vertical plane, even though the distances involved may be different for the two planes.

We have here a prescription for determining the focal properties of a given combination of quadrupoles. The experimenter is usually faced with the opposite problem, how to find the quadrupole strengths that will accomplish a given focusing. In practice this is usually accomplished by a process of trial and error. The graphs shown in Figures 9, 10, and 11 may be used for rapid rough calculations for both planes of focusing. To describe the method of reaching the desired values of L_1 and L_2 for specified object and image distances in each plane, we call plane I the plane in which quadrupole 1 is focusing, and plane II that in which quadrupole 2 is focusing. For plane I a value of L_2 is assumed (usually about 0.8) and the graphs are used to calculate backward through quadrupole 2 from the desired image distance so that L_1 may be chosen for the desired object distance. In plane II the calculation is carried forward through the system, keeping L_1 as previously determined but adjusting L_2 to give the desired image distance. The calculation is then again carried backward in plane I, L_1 being adjusted to the proper object distance, and the cycle carried on until adequate accuracy is achieved. The recommended order of calculations is chosen to take advantage of the fact that in a given plane the focusing lens has a much more dominant effect than the defocusing lens. Thus, the suggested order gives a rapid convergence to the desired conditions. The use of the graphs usually allows obtaining L_1 and L_2 to within less than 10 per cent. Actual computation, again by trial, should allow determining the quadrupole characteristics for a given problem to 1 per cent.

For quadrupole triplets the procedure is not much different except that it is less convenient to use the reduced object and image distance P' and Q' because the effective lengths l of the quadrupole components are not usually

problem to 1 per cent.

For quadrupole triplets the procedure is not much different except that it is less convenient to use the reduced object and image distance P' and Q' because the effective lengths l of the quadrupole components are not usually equal for all elements of the triplet. The expressions involving p' and q' are more convenient. The first and last quadrupoles of a triplet are frequently identical and are operated at the same magnetization.

Hand & Panofsky (10) have developed a rectangular quadrupole, on the basis of a suggestion by O. Piccioni. The field pattern is the same as that of the conventional quadrupoles already discussed, but it is available in rectangular, rather than square or round, cross section. The rectangular quadrupole is suggested because conventional quadrupoles cannot usually be used to full aperture except in the focusing plane. By using a rectangular quadrupole, with larger aperture in the focusing plane, one avoids producing some unused region of field. Whether rectangular quadrupoles have economic advantages over conventional quadrupoles is difficult to determine at this time.

Sternheimer (11) has made extensive calculations for a double-focusing magnet system that combined, in the same components, the functions of deflecting magnet and quadrupoles. Non-uniform fields are used. Instruments of this type may be expected to be extremely useful in the future, especially for short-lived particles; however, they are somewhat less flexible than instruments in which the deflecting and focusing functions are separated.

MATRIX METHOD FOR COMBINING COMPONENTS

Matrices may also be used to advantage, especially if the computation is to be adapted to a digital computer. The y and z co-ordinates of an orbit with the respect to the lens axis (x axis) may be treated separately. Taking, for example, the y co-ordinates, one can represent the position and slope of an orbit as a column symbol

$$\begin{bmatrix} y \\ \dfrac{dy}{dx} \end{bmatrix}_{x=0}$$

at a given point in the system, here taken as $x=0$. A field-free region of length b is represented by the matrix

$$\begin{pmatrix} 1 & b \\ 0 & 1 \end{pmatrix} \quad \text{(field-free length } b)$$

in that the new y co-ordinate and slope dy/dx are given by the matrix equation

$$\begin{bmatrix} y \\ \dfrac{dy}{dx} \end{bmatrix}_{x=b} = \begin{bmatrix} 1 & b \\ 0 & 1 \end{bmatrix} \begin{bmatrix} y \\ \dfrac{dy}{dx} \end{bmatrix}_{x=0}$$

Similarly, the matrix giving the values of y and dy/dx at the exit effective end of a quadrupole in terms of the corresponding values at the entrance effective end is, for the focusing plane,

$$\begin{pmatrix} \cos(kl) & (1/k)\sin(kl) \\ -k\sin(kl) & \cos(kl) \end{pmatrix}$$

and, for the defocusing plane,

$$\begin{pmatrix} \cosh(kl) & (1/k)\sinh(kl) \end{pmatrix}$$

$$\begin{pmatrix} y \\ dy \\ dx \end{pmatrix}_{x=b} = \begin{pmatrix} 1 & 0 \\ 0 & 1 \end{pmatrix} \begin{pmatrix} y \\ dy \\ dx \end{pmatrix}_{x=0}$$

Similarly, the matrix giving the values of y and dy/dx at the exit effective end of a quadrupole in terms of the corresponding values at the entrance-effective end is, for the focusing plane,

$$\begin{pmatrix} \cos(kl) & (1/k)\sin(kl) \\ -k\sin(kl) & \cos(kl) \end{pmatrix}$$

and, for the defocusing plane,

$$\begin{pmatrix} \cosh(kl) & (1/k)\sinh(kl) \\ k\sinh(kl) & \cosh(kl) \end{pmatrix}$$

As an example of the use of these matrices, we give the matrix applicable to the following situation: from the starting point there is first a field-free region of length b to the entrance-effective end of a focusing quadrupole of effective length l and strength parameter k_1, followed by effective gap g, and finally by a defocusing quadrupole of the same effective length l and strength parameter k_3. The combined matrix is

$$\begin{pmatrix} \cosh(k_3l) & (1/k)\sinh(k_3l) \\ k\sinh(k_3l) & \cosh(k_3l) \end{pmatrix} \begin{pmatrix} 1 & g \\ 0 & 1 \end{pmatrix} \begin{pmatrix} \cos(k_1l) & (1/k)\sin(k_1l) \\ -k\sin(k_1l) & \cos(k_1l) \end{pmatrix} \begin{pmatrix} 1 & b \\ 0 & 1 \end{pmatrix}$$

with

$$k = (\alpha/B\rho)^{1/2} = [(dB/dr)/B\rho]^{1/2}$$

The matrix above will be taken to have the form

$$\begin{pmatrix} a_1 & a_2 \\ a_3 & a_4 \end{pmatrix}$$

If we assume the object is at the original starting point, this matrix has the form

$$\begin{pmatrix} m + (q'/f) & -(q'/m) \\ -(1/f) & (1/m) \end{pmatrix}$$

where m is the magnification of the image formed, q' is the distance to this image, and f is the focal length of the combined lens. Therefore, the distance q' from from the exit-effective end to the image is

$$q' = -(a_2/a_4)$$

and the magnification is

$$m = (1/a_4)$$

The form of the matrix relating the column symbol at image position to the column symbol at object position must be

$$\begin{pmatrix} m & 0 \\ -(1/f) & (1/m) \end{pmatrix}$$

In general, when quadrupoles are to be adjusted to perform a desired focusing operation in both the y co-ordinate and the z co-ordinate, a method of successive approximations must be used.

USE OF WIRE ORBITS TO TEST COMPONENTS

A current-carrying wire that is under tension takes up a position coincident with the orbit of a charged particle in a magnetic field, provided the current and tension of the wire are adjusted to correspond to the momentum of the particle in question. The current I (amps) in the wire and tension T (grams of force) must satisfy the condition

$$I(\text{in amp.})/T(\text{in gm.}) = 2.94/p(\text{in Mev/c})$$

and the current I must flow in the direction opposite to the beam current represented by the charged particles moving along the orbit. The outline of a brief derivation follows.

Using Gaussian cgs units, one finds the force dF on a small length ds of a wire carrying current I in magnetic flux density B is

$$dF = -I\,ds \times B$$

The minus sign in the expression above reflects the opposite sense of I and s. Using t as a unit vector tangent to the wire, we readily obtain

$$dt/ds = (I/T)t \times B$$

A similar equation may be derived for the orbit of a charged particle if t is now used to represent the unit vector tangent to the orbit. Again in Gaussian units, the force F on a particle with charge e and velocity v is

$$F = (e/c)v \times B = dp/dt$$

The following expressions outline the steps;

$$|p| = p = \text{const. magnitude of momentum}$$
$$ds = v\,dt$$
$$t = p/p = v/v$$
$$(e/c)v \times B = (ev/c)t \times B = v\,dp/ds = vp\,dt/ds$$
$$dt/ds = (e/pc)t \times B \qquad (\text{Gaussian units})$$

The equations for wire and orbit are identical provided we have

$$I/T = e/pc \qquad (\text{in Gaussian units})$$

Measuring wire current I in amperes, tension T in grams of force ($g = 980$ cm./sec.²), taking e as one (positive) electron charge, and measuring p in Mev/c give the expression at the beginning of this section. The weight of the wire is neglected here.

The current-carrying wire allows easy visualization of particle trajectories through a magnetic system. With measuring microscopes, accurate

(m, s/c), taking e as one (positive) electron charge, and measuring p in Mev/c give the expression at the beginning of this section. The weight of the wire is neglected here.

The current-carrying wire allows easy visualization of particle trajectories through a magnetic system. With measuring microscopes, accurate information about focusing properties may be obtained. Using a carefully balanced pulley wheel located at the source or apparent source of particles, with weights to give the desired wire tension, one may use the wire to find accurate data on the focal length of a magnet system. It is not feasible to extend the wire all the way to the focus point because the wire then becomes unstable. The wire is held fixed at some movable support short of the focus point, and wire positions are recorded at two points along the wire in the field-free region outside the magnet system. A number of wire positions must be used to determine the focus point to which the orbits converge.

Figure 13 shows the arrangement for measuring the focal properties of a pair of quadrupoles, showing two positions of the current-carrying wire. In some cases two wires carrying the same current in the same direction may be used to advantage. The focus point is determined by straight-line extrapolation of the orbits in the field-free region.

Careful measurements with wire orbits can give valuable information about aberrations, especially in arrangements such as those involving electric deflection to separate particles of differing mass. A suitable current regulator has been described by Lutz & Pike (12).

EXAMPLES OF PURELY MAGNETIC SYSTEMS

A simple system for obtaining a negative pion beam at 1.4 Bev/c has been used by Chretien,Leitner, Samios, Schwartz & Steinberger (13). Their focusing and momentum selection were provided by the magnetic field of the Cosmotron. Where an image of the target was formed they inserted a collimator to provide momentum selection. No great intensity was needed for their bubble chamber; but they required, and obtained, momentum selection within about 1 per cent accuracy. The arrangement is shown in Figure 14.

A single spectrograph magnet of very considerable usefulness has been made by Crewe (14). It uses a uniform field, and can be used up to about 10,000 gauss, with focusing provided purely by sloping and curving the pole edge at entrance and exit. It provides a focus only in the central plane (which we refer to as horizontal even though it is not horizontal in the Crewe design). In the vertical plane it does not focus, but because of some vertical focusing at the entrance to the magnet it preserves a good effective solid angle for particles leaving the target. The magnet involves bending by 60 degrees. Reference (14) gives a worthwhile discussion of the design considerations. Similar principles have been used by Meier, Fletcher, Wisseman & Williamson (15).

A very useful spectrometer based on uniform magnetic field has been constructed by Lovati & Tyren (16). Their instrument has focusing in both planes.

Browne & Buechner (17) have discussed the use of a magnet with uniform field and round pole pieces to allow focusing, as a spectrograph, for a wide band of momenta. A refinement of the same type of instrument is described by Enge (18), in which a single quadrupole is introduced to give a greatly increased effective solid angle.

A series of important experiments has been done by Hofstadter and others with a magnetic spectrograph based on a non-uniform field and 180-degree bending. A brief description of one model has been given by Hofstadter,

by Enge (18), in which a single quadrupole is introduced to give a greatly increased effective solid angle.

A series of important experiments has been done by Hofstadter and others with a magnetic spectrograph based on a non-uniform field and 180-degree bending. A brief description of one model has been given by Hofstadter, Fechter & McIntyre (19). A more complete description of this general type of magnet may be seen in the article of Snyder, Rubin, Fowler, and Lauritsen (20).

A double spectrograph, essentially one spectrograph followed by a second spectrograph, has been used in the antiproton work of Chamberlain, Segre, Wiegand & Ypsilantis (21) and has been discussed previously in this Review (22). A later version utilizing the same principles has been described by Elioff, Agnew, Chamberlain, Steiner & Ypsilantis (23) and is shown in Figure 15. The magnetic analysis is provided by the deflecting magnets $M1$ and $M2$, and the focusing by quadrupole triplet lenses $Q1$, $Q2$, and $Q3$. The target T is first focused at the position of the scintillation counter $S1$, where there is considerable dispersion, so that the counter acts to select a narrow momentum band about the central momentum near 1.5 Bev/c. The second spectrograph, involving $Q2$ and $M2$, forms a second focus at the counters $S2$, $\check{C}SC$ II, and $\check{C}$. The momentum dispersion of the first spectrograph is compensated by that of the second spectrograph so that all particles accepted by the first spectrograph fall into a reasonably small image at $S2$. The momentum was defined to ± 3 per cent, and the image size at $S2$ was 4.5 cm. high by 7 cm. wide. The final lens $Q3$ focused the beam into the experimental area A. Helium-filled plastic bags were inserted in the spectrograph over most of its length, to reduce the multiple scattering that would otherwise be caused by air. Antiprotons were selected (from the beam that was mostly composed of mesons and electrons) by both a Cerenkov counter and time-of-flight measurement.

Owing to finite size of target and deviation of the momentum from the central momentum, there is a loss of particles that fail to enter the aperture of the second spectrograph in the arrangement of Figure 15, even for particles within the desired band of momenta. Piccioni (24) has pointed out that the loss may be reduced by installing a field lens close to $S1$. Such a lens would be arranged to focus the aperture of $Q1$ onto the aperture of $Q2$. In the apparatus of Figure 15 there was so much multiple scattering by $S1$ at the first focus that the field lens would not be expected to help the transmission of the system materially. However, the concept of the field lens has been used to great advantage in other arrangements.

The use of field lenses can be extended to give a series of lenses that successively focus and refocus the beam even if the beam includes a fairly broad band of momenta. Such a system, used in connection with antiproton experiments, is shown in Figure 16. It is taken from the work of Cork, Lambertson, Piccioni & Wenzel (25), who have given a readable description of their arrangement of magnets. Antiprotons were selected purely on the basis of time-of-flight measurements.

For the handling of the beam from a linear electron accelerator, Panofsky & McIntyre (26) have devised a useful system for providing momentum analysis without introducing dispersion in the final image. Their paper is recommended reading because of the insight it gives into their design considerations.

MEASUREMENT OF TRANSMISSION OF A MAGNETIC BEAM-FORMING SYSTEM

The typical magnetic system we are discussing is intended to form a secondary beam of particles from the particles emerging from a target. The number of particles in the secondary beam is usually proportional to what we will call the acceptance A, which may be written as the product of a solid angle Ω, referring to the solid angle in which particles may leave the target and still be contained in the secondary beam, and a momentum Δp, loosely called "momentum bite":

$$A \cong \Omega \Delta p$$

In most cases the acceptance A is not simply the product of the maximum solid angle and the momentum spread of the resultant beam. Rather, the solid angle in which particles may be accepted is a function of the momentum p of the particles, and the acceptance is defined as

$$A = \int_{p_{min}}^{p_{max}} \Omega(p) dp$$

It is frequently unnecessary to measure or calculate the solid angle function $\Omega(p)$, but it is important to know the acceptance A. One example is the early antiproton experiment, in which it was desired to have some estimate of the absolute antiproton yield. This involved knowing the acceptance of the system and the number of antiprotons passing through the system for a given number of high-energy protons hitting the (primary) target.

If the system is very simple and involves only one focus point of the particles, then the problem is relatively simple. Figure 17 shows such an example. It is assumed that the target represents a "white" source because a broad band of momenta is emitted by the target into a solid angle large compared to the solid angle subtended by the lens aperture. Then the rate at which particles pass through the system (i.e., the counting rate) is proportional to the acceptance of the system. By temporarily installing a variable collimator and a narrow slit (or narrow counter) at or near the first focus point, one may measure the counting rate under conditions for which the acceptance is

$$A = \Omega_{coll} \Delta p_{slit}$$

where Ω_{coll} is the solid angle subtended at the target by the collimator aperture and Δp_{slit} is the momentum interval corresponding to the slit width for a ray that is initially a central ray (passing through target center and collimator center). For the example in Figure 17, where the analyzing magnet is used near minimum deviation one may use the expression

$$\Delta p_{slit} = p(\Delta\theta/\theta)$$

where p is the particle momentum for which the system is adjusted, θ is the bending angle at the analyzing magnet, and $\Delta\theta$ is the interval of θ determined

a ray that is initially a central ray (passing through target center and collimator center). For the example in Figure 17, where the analyzing magnet is used near minimum deviation one may use the expression

$$\Delta p_{slit} = p(\Delta\theta/\theta)$$

where p is the particle momentum for which the system is adjusted, θ is the bending angle at the analyzing magnet, and $\Delta\theta$ is the interval of θ determined by the edges of the vertical slit at the focus point.

Once the counting rate has been determined for conditions of known acceptance (i.e., with collimator and slit, as discussed above), the acceptance of the system with collimator and slit removed may be known simply by measuring the counting rate, for the acceptance is directly proportional to the counting rate of particles through the system.

More complicated systems are frequently used, in which the secondary beam may be focused and refocused at several points along the system. Usually the acceptance is a function of how well the various components are matched to one another. In measuring the over-all acceptance it is good practice to compare the counting rate through the complete system with the rate at which particles reach the first focus when the collimator and slit are in place as described above. This simple procedure should be adequate even for complicated systems with aperture stops at many points along the system.

When a monochromatic initial beam is to be used in evaluating the acceptance of a magnetic system, a ribbed absorber can frequently be used at the position usually occupied by the target to give a "white" spectrum and to give sufficient multiple scattering to cause the entrance to the magnetic system to be rather uniformly illuminated. One form of ribbed absorber is shown in Figure 18. The ribs must be deep enough to give a momentum spread to the emerging particles that is guaranteed to be greater than the momentum spread of the beam that normally would pass through the system. Each rib should be quite narrow compared with the width of the incident beam.

ABERRATIONS

Chromatic aberration tends to be present in any system of quadrupole lenses. For a single lens, a given fractional change of momentum is usually reflected in a fractional change of effective focal length 1.5 to 4 times as great, i.e., $\Delta f/f \approx (1.5$ to $4)(\Delta p/p)$. Of course, chromatic aberrations can be calculated by the procedures previously described, providing a particle momentum slightly different from the central momentum is used in the calculation.

Geometrical aberrations are failures of focus related to finite object size and finite angular aperture. For bending magnets aberrations may appear in second order, while for a pure quadrupole system the third-order aberrations should be the lowest order to appear.

For bending magnets the second-order spherical aberration can be eliminated for the horizontal plane (27), and, in fact, perfect focusing may be achieved in the horizontal plane—as was pointed out for example, by Kerwin (28) and by Kerwin & Geoffrion (29). However, it is not possible to eliminate all second-order aberrations simultaneously, including those in the vertical plane.

For purely quadrupole components, second-order aberrations should be absent to the extent that quadrupole symmetry is maintained. The third-order aberrations are extremely complicated, involving some 20 Seidel coefficients.

Kerwin (28) and by Kerwin & Geoffrion (29). However, it is not possible to eliminate all second-order aberrations simultaneously, including those in the vertical plane.

For purely quadrupole components, second-order aberrations should be absent to the extent that quadrupole symmetry is maintained. The third-order aberrations are extremely complicated, involving some 20 Seidel coefficients.

SEPARATED BEAMS

Given a magnetic system that provides a charged-particle beam of well defined momentum, one may separate out particles of a particular mass by sorting the particles on the basis of their velocities. A number of methods have been suggested. We describe here one of the most successful forms of apparatus for achieving the separation, the parallel-plate electrostatic separator. It was first used for particles of high energy by Coombes, Cork, Galbraith, Lambertson, & Wenzel (30). Whereas deflection in a magnetic field depends on particle momentum, being proportional to $1/p$, deflection in an electric field depends upon momentum times velocity, and is proportional to $1/pv$.

The magnetic selection of momenta involves deflection in the horizontal plane, as in the systems described previously. The electric deflection occurs in the vertical plane, with a vertical electric field obtained by applying high voltage to electrodes above and below the beam of secondary particles. In its simplest form such a system is shown in Figure 19. Figure 19a shows the plan view. Figure 19b shows the focal properties of the system for deviations in the horizontal plane and for the central momentum only. In that plane the separator has no effect. Figure 19c shows the focusing properties in the vertical plane. The vertical electric field between the parallel plates of the separator causes a deflection, usually very small, in the vertical plane. The curvature (in cm.$^{-1}$) of the trajectory in the transverse electric field is given by the expression

$$K = \frac{E(\text{in v/cm.})}{p(\text{in Mev/c})^2} \times 10^{-6}$$

As a result of the electric field, particles of differing velocity have different vertical focus positions at the final slit, and a narrow slit may be used to exclude all except the particles of a chosen velocity.

So far, we have described the separated beam only in a rudimentary form. A number of refinements are necessary if one is to achieve the best available performance:

(a) Since it is important to get considerable separation of particles of differing masses on the basis of a small electric deflection, the target is made extremely small in the vertical dimension, perhaps 2 mm.

(b) To avoid the multiple scattering involved in passing the beam through vacuum windows, the whole system may be made with a vacuum system common to the accelerator.

(c) The focusing properties are chosen to eliminate, as much as possible, the particles that have scattered from the walls of the vacuum system.

(d) In the region of the separator (where there is a vertical electric field), a small horizontal magnetic field is also applied. This makes the arrangement into a Wien filter. In the resulting system there is no deflection due to the separator for particles of the desired velocity, but faster or slower particles are deflected upward or downward. This choice allows all the magnet components except the separator to be adjusted before the separator is turned on.

(e) Care is given to the shaping and spacing of the "parallel-plate" electrodes to give a strictly uniform vertical component of electric field, at least to a few per cent.

(f) One of the magnets, usually the deflecting magnet, is carefully shimmed for the purpose of making the vertical focus as good as possible, particularly with respect to chromatic aberrations. This process usually involves great care in the use of wire orbits to measure the aberrations. The vertical focusing properties are improved at the sacrifice of the properties in the horizontal plane, which need not be nearly as good.

(g) A small series of counters is located close to the slit but above or below the desired beam to show the spatical shape and position of the focus of one of the undesired (but copious) components of the beam. This series of counters allows constant checks on the adjustment of the separator and on the focusing properties of the magnetic system.

(h) Frequently two or more stages of separation are used to obtain better over-all separation and to prevent the system's being "fooled" by particles that suffer a decay process while passing through the system.

An extraordinarily good separated beam with parallel-plate separators has been set up by Eberhard, Good & Ticho (31). It was designed to give a separated beam of K^- mesons of momentum 1.2 Bev/c for a liquid-hydrogen bubble chamber. Two successive stages of separation were used to reject negative pions by a factor of 10^5. The vertical dimension of the target was 3 mm. The spacing between parallel-plate electrodes was 6.3 cm, and the potential difference between electrodes was 380 kv. Reference (31) describes many of their design considerations, some of which have been outlined above. The quality of the beam may be summarized by stating the relative numbers of K^-, π^-, and μ^- as 1:0.06:1, whereas at the target there was a ratio $K:\pi$ of 1:140.

A coaxial Wien-filter separator has been used by Horwitz, Miller, Murray & Tripp (32). The separator has been described an in unpublished report by Murray (33). At present, it appears that the parallel-plate separators may be more useful than the coaxial separators simply because the parallel-plate construction is simpler.

A new form of separator, called a septum separator, has been proposed

be more useful than the coaxial separators simply because the parallel-plate construction is simpler.

A new form of separator, called a septum separator, has been proposed by Murray (34). It involves many plane electrodes spaced very closely in vacuum, with alternate electrodes connected to high positive and negative voltage supplies. As with the other separators, a transverse magnetic field would be applied to make a Wien filter. Unwanted particles would be stopped by absorption in the plates of the separator. The advantage of the septum separator is that high electric fields (200 kv./cm. over 0.16 cm. gap) can be used, making shorter separators possible. The disadvantage is its inherently poor geometrical transmission. It is not yet fully evaluated experimentally.

Preliminary work by Murray (35) shows that higher fields can be maintained in a parallel-plate separator if the negative electrode is coated with slightly conducting glass. The glass serves to quench sparks locally before a strong discharge can develop. The glass surface has not yet been tested in a full-size separator.

Radio-frequency fields can be used, instead of d.c. fields, to achieve separation of particles of different mass. A number of distinct modes of operation have been proposed. One method involves using a primary beam, from an accelerator, that is modulated rapidly and periodically in time, such as the beam from an electron accelerator that uses microwave acceleration. By passing the magnetically analyzed secondary beam through a synchronized radio-frequency (r.f.) field, one may achieve a separation of the components of the beam of different velocities because the different-speed components of the secondary beam have different times of flight between the target and the r.f. field region. Such a system has been described by Panofsky (36). In the same paper the focusing properties of an interesting spectrograph are illustrated.

Another mode of operation of an r.f. separator involves using a long r.f. cavity. The field in the cavity is visualized in terms of traveling waves reflecting from the ends of the cavity. The phase velocity of the cavity is adjusted to match the velocity of some unwanted component in the beam, such as the pions in an antiproton beam. The pions then suffer a deflection due to the r.f. field. The length of the cavity is chosen so that there is no net deflection of the desired (antiproton) beam component, by arranging the length so that the desired component falls behind (or ahead of) the r.f. traveling wave by an integral number of full wavelengths during the transit through the cavity. A recent proposal of this type has been made by Blewett (37).

The simplest use of an r.f. cavity would seem to be in a TE mode, with the electric field transverse to the beam direction. However, Panofsky & Wenzel (38) have pointed out that in such a mode the magnetic field cancels the deflection due to the electric field. Either a TM mode must be used, or a special cavity configuration such as that discussed by Blewett (37).

Until now the r.f. separators have not been thoroughly tried in practice; therefore, no complete analysis is attempted here.

EXTREMELY CLEANLY COLLIMATED BEAMS

In some experiments it is of no consequence if there is a very small fraction of the beam spread rather widely in space, but in other experiments it is quite crucial that the beam be very well confined to a given region. In general, strong focusing has been a great help toward clean beams but special precautions are still necessary in special cases, such as separated beams.

In some experiments it is of no consequence if there is a very small fraction of the beam spread rather widely in space, but in other experiments it is quite crucial that the beam be very well confined to a given region. In general, strong focusing has been a great help toward clean beams but special precautions are still necessary in special cases, such as separated beams.

Considerable care was given to the problem of a clean beam by Eberhard, Good & Ticho (31). Another very elegant example is the so-called pencil beam of protons from the Cosmotron used by Cool, Morris, Rau, Thorndike & Whittemore (39) to produce strange particles within a diffusion cloud chamber while leaving most of the chamber free from unwanted tracks. Both these papers give some description of design methods.

No attempt is made in this article to give a complete description of methods of producing very clean beams. However, a few comments can be made. It is very helpful to be able to use a geometrically small target, since the desired beam can then be passed, with careful focusing, through relatively narrow slits. It pays to place the important collimators fairly early in the system. Particles that have been degraded in energy in passing through the walls of a collimator can be effectively rejected if one of the last components of the beam-forming system is a deflecting magnet with large pole separation. It is frequently important to use collimators that are rather thin in the beam direction to reduce the number of particles that scatter from the inside collimator wall. A collimator need not be very thick, if it is followed by considerable magnetic bending, to reject particles that have lost appreciable energy in the collimator material.

191. Ann Rev Nuc Sci., 154 p47 DAA-4

1. Cranam, E. D., Livingston, M. S., and Snyder, H. S., *Phys. Rev.*, 88, 1190 (1952)

2. Rankin, B., *Rev. Sci. Instr.*, 25, 675 (1954)

3. Fermi, E. (Personal communication, 1949)

4. Cross, W. G., *Rev. Sci. Instr.*, 22, 717 (1951)

5. Bainbridge, K. T., *Experimental Nuclear Physics*, Part V, I, 559 (Segrè, E., Ed., John Wiley & Sons, Inc., New York, N. Y., 789 pp., 1953)

6. Buechner, W. W., *Progr. in Nuclear Phys.*, 5, 1 (1956)

7. Judd, D. L., *Rev. Sci. Instr.*, 21, 213 (1950)

8. Sternheimer, R. M., *Rev. Sci. Instr.*, 23, 629 (1952)

9. Seal, D. H. (Personal communication, 1959)

10. Hand, L. N., and Panofsky, W. K. H., *Rev. Sci. Instr.*, 30, 927 (1959)

11. Sternheimer, R. M., *Rev. Sci. Instr.*, 24, 573 (1953)

12. Lutz, L., and Pike, C., *Rev. Sci. Instr.*, 30, 811 (1959)

13. Chretien, M., Leitner, J., Samios, N. P., Schwartz, M., and Steinberger, J., *Phys. Rev.*, 103, 383 (1957)

14. Crewe, A. V., *Rev. Sci. Instr.*, 29, 380 (1958)

15. Meier, O. Jr., Fletcher, N. R., Wasserman, W. R., and Williamson, R. M., *Rev. Sci. Instr.*, 29, 1004 (1958)

16. Lovati, A., and Tyrén, H., *J. Sci. Instr.*, 33, 151 (1956)

17. Browne, C. P., and Buechner, W. W., *Rev. Sci. Instr.*, 27, 899 (1956)

18. Inge, H. A., *Rev. Sci. Instr.*, 29, 885 (1958)

19. Hofstadter, R., Fechter, H. R., and McIntyre, J. A., *Phys. Rev.*, 92, 978 (1953)

20. Snyder, C. W., Rubin, S., Fowler, W. A., and Lauritsen, C. C., *Rev. Sci. Instr.*, 21, 852 (1950)

21. Chamberlain, O., Segrè, E., Wiegand, C., and Ypsilantis, T., *Phys. Rev.*, 100, 947 (1955)

22. Segrè, E., *Ann. Rev. Nuclear Sci.*, 8, 127 (1958)

23. Eliot, T., Agnew, L., Chamberlain, O., Steiner, H., Wiegand, C., and Ypsilantis, T., *Phys. Rev. Letters*, 3, 285 (1959)

24. Piccioni, O. (Personal communication, 1956)

25. Cork, B., Lambertson, G. R., Piccioni, O., and Wenzel, W. A., *Phys. Rev.*, 107, 218 (1957)

26. Panofsky, W. K. H., and McIntyre, J. A., *Rev. Sci. Instr.*, 25, 287

(1958)

23. Elioff, T., Agnew, L., Chamberlain, O., Steiner, H., Wiegand, C., and Ypsilantis, T., *Phys. Rev. Letters*, **3**, 285 (1959)

24. Piccioni, O. (Personal communication, 1956)

25. Cork, B., Lambertson, G. R., Piccioni, O., and Wenzel, W. A., *Phys. Rev.*, **107**, 248 (1957)

26. Panofsky, W. K. H., and McIntyre, J. A., *Rev. Sci. Instr.*, **25**, 287 (1954)

27. Bainbridge, K. T., *Proceedings of the Seventh Solvay Conference*, 55 (Briggs, R., Ed., Brussels, Belgium, 441 pp., 1948)

28. Koewin, L., *Rev. Sci. Instr.*, **20**, 36 (1949)

29. Koewin, L., and Gourton, C., *Rev. Sci. Instr.*, **20**, 384 (1949)

30. Coombes, C. A., Cork, B., Galbraith, W., Lambertson, G. R., and Wenzel, W. A., *Phys. Rev.*, **112**, 1304 (1958)

31. Eberhard, P., Good, M. L., and Ticho, H. K., *U. S. Atomic Energy Commission Doc.*, *UCRL-8878 Rev.*, 25 pp. (1959); or *Rev. Sci. Instr.* (To be published)

32. Horwitz, N., Miller, D., Murray, J., and Tripp, R., *Phys. Rev.*, **115**, 472 (1959)

33. Murray, J. J., *U. S. Atomic Energy Commission Doc.*, *UCRL-3492*, May 1957 (Unpublished)

34. Murray, J. J. (Personal communication, 1959)

35. Murray, J. J. (Personal communication, 1959)

36. Panofsky, W. K. H., *Proc. Intern. Conf. High Energy Accelerators and Instrumentation, CERN, 1959*, 428 (Kowarski, L., Ed., CERN, Geneva, Switzerland, 705 pp., 1959)

37. Blewett, J. P., *Proc. Intern. Conf. High Energy Accelerators and Instrumentation, CERN, 1959*, 422 (Kowarski, L., Ed., CERN, Geneva, Switzerland, 705 pp., 1959)

38. Panofsky, W. K. H., and Wenzel, W. A., *Rev. Sci. Instr.*, **27**, 967 (1956)

39. Cool, R. L., Morris, T. W., Rau, R. R., Thorndike, A. M., and Whittemore, W. L., *Phys. Rev.*, **108**, 1048 (1957)

Upper coil

Iron

Lower coil
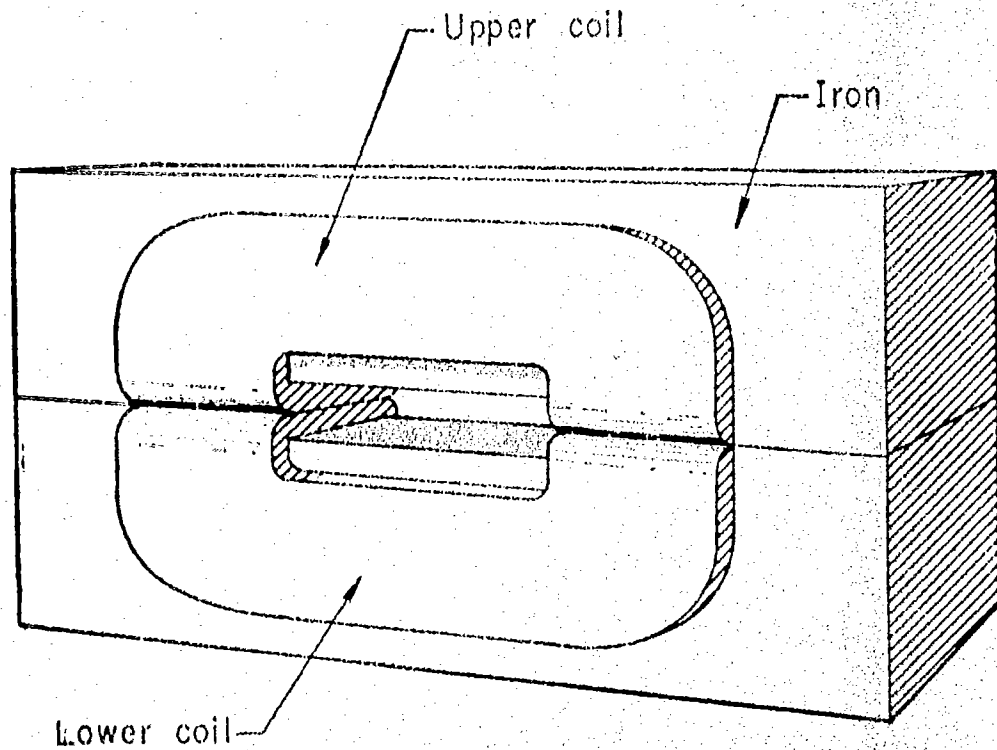
FIG. 1. General-purpose deflecting magnet. This arrangement, with so-called "window-frame" construction, has proved very useful because it gives a very uniform field even close to the coils and may be used as high magnetic flux densities.

N   S

S   N
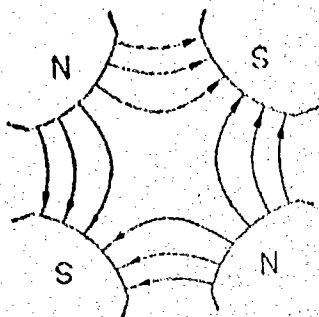
FIG. 2. Field pattern of a quadrupole magnet.
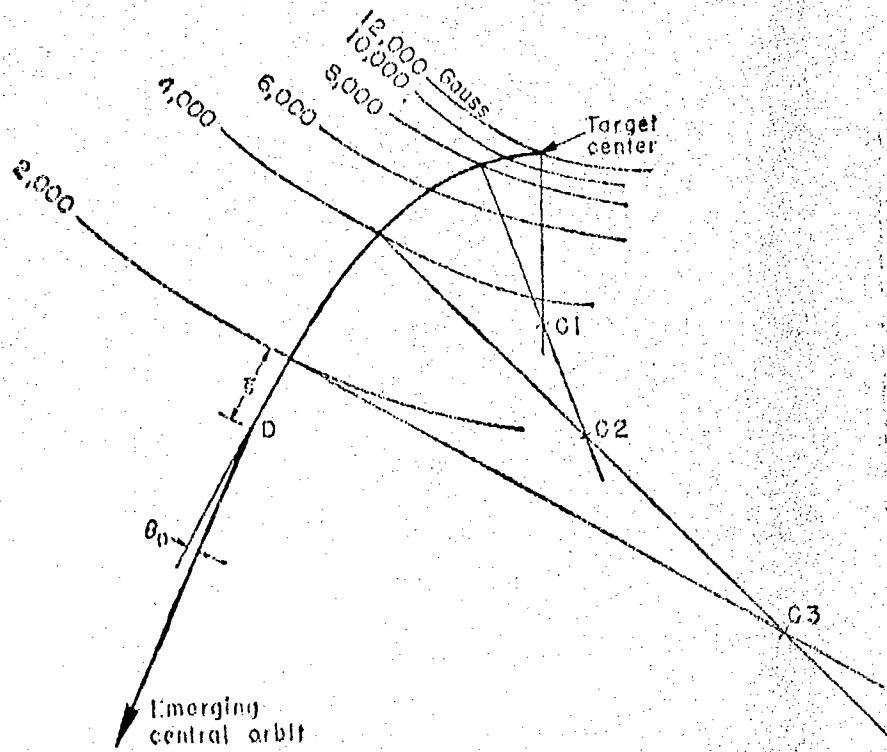
Fig. 3. Example of the graphical tracing of the orbit of a charged particle in the central plane. The orbit is approximated by a succession of circular arcs. This example is carried out in unusually coarse steps. See text for details.
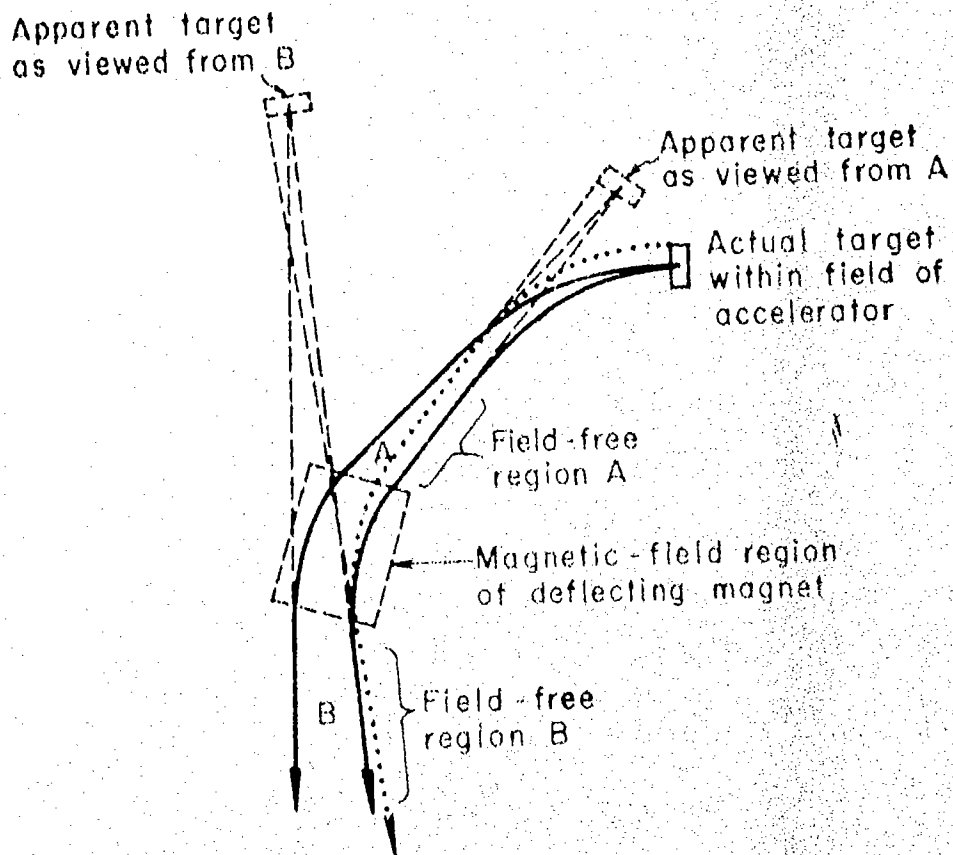
Fig. 4. Diagram of orbits illustrating the determination of position and horizontal size of the apparent target. Solid lines are used to represent orbits originating at the target center. The dotted line shows an orbit from the edge of the target. Dashed lines show extrapolation back to the apparent target. In some cases the apparent target may be quite different in size from the actual target.
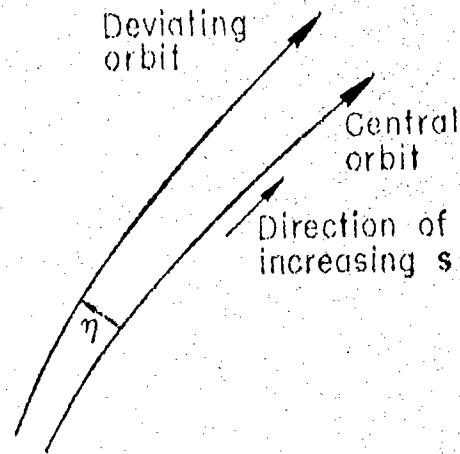
FIG. 5. Diagram illustrating the parameter η, the lateral displacement of an orbit from the central orbit. Here η is positive as drawn if the z axis is directed up out of the plane of the figure.
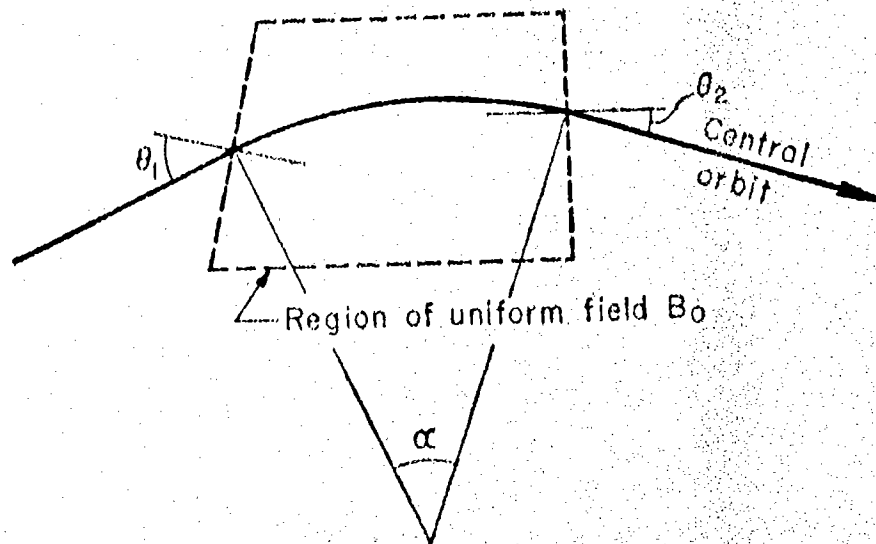
FIG. 6. Definition of the angles θ_1, θ_2 and α used in the text. The angles are considered positive as drawn.
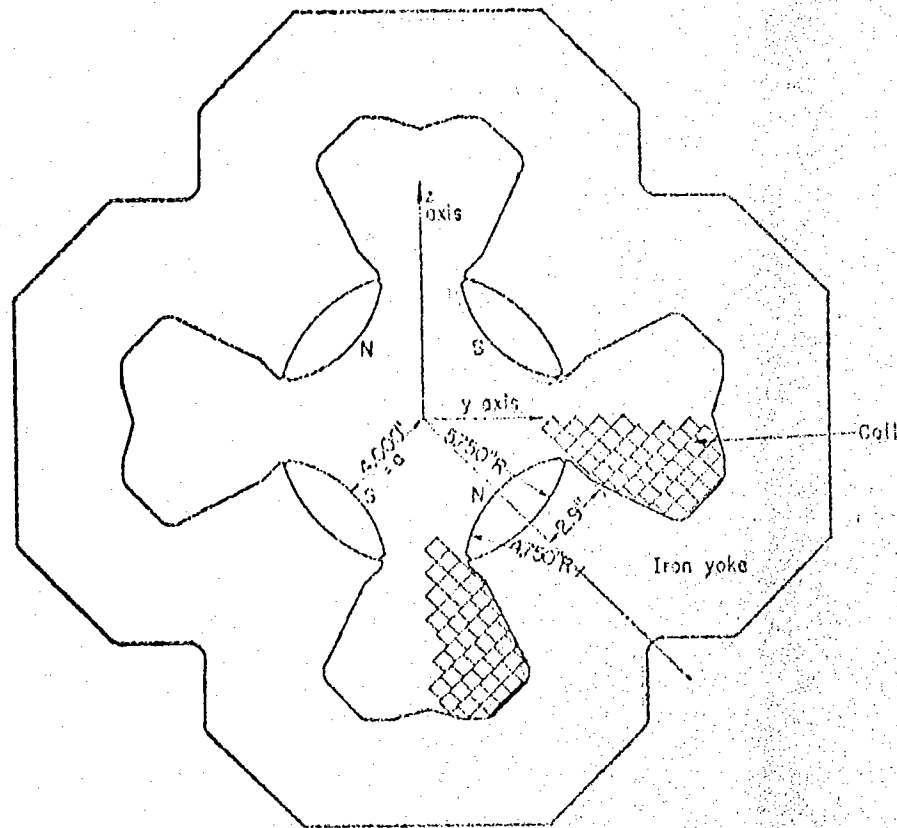
Fig. 7. Quadrupole magnet, showing the cross section, to scale, of one of the most satisfactory quadrupole varieties. Important dimensions are indicated.
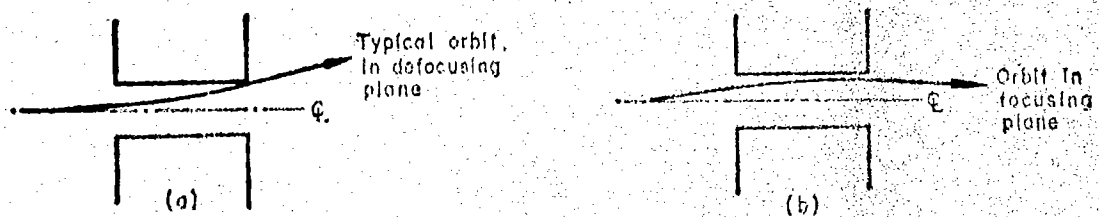
Fig. 8. Side and top views of quadrupole aperture showing a typical orbit that is off the axis.
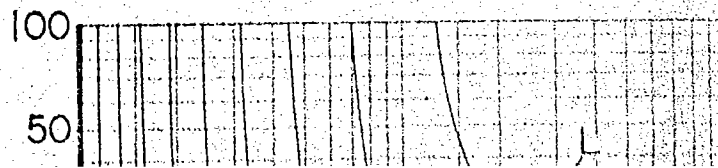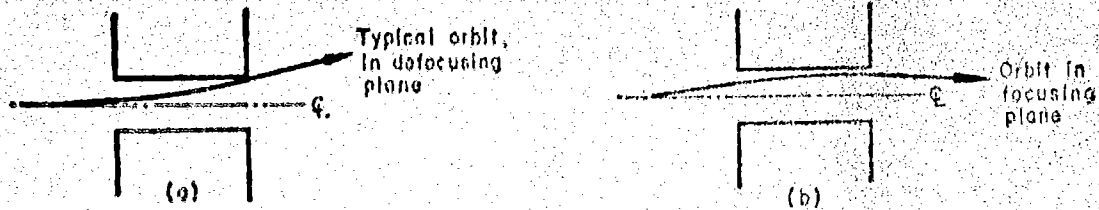
FIG. 8. Side and top views of quadrupole aperture showing a typical orbit that is off the axis.
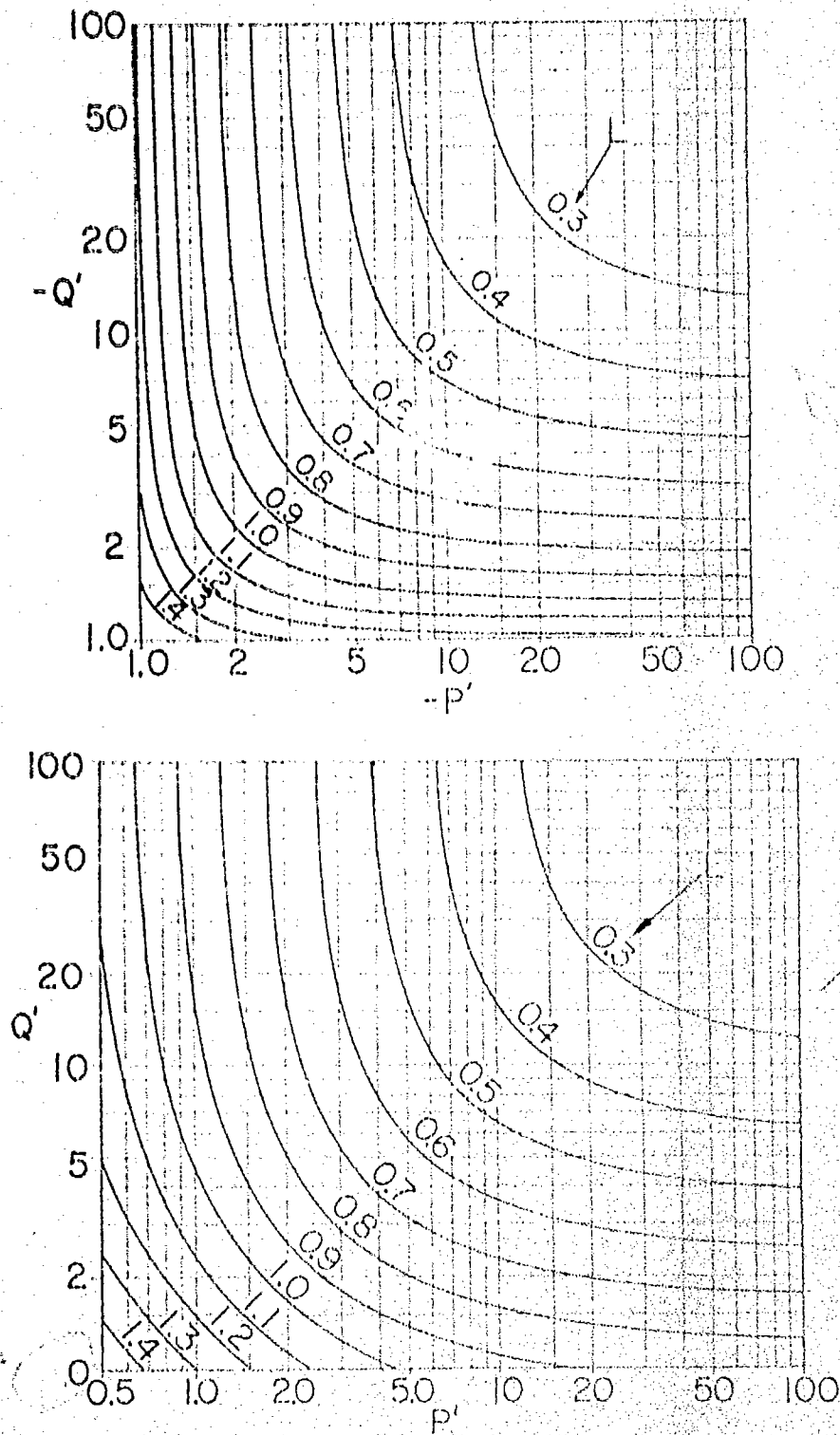
FIG. 9. Graphical presentation of quadrupole optics. The reduced image distance Q' and magnification m are given as functions of reduced object distance P' for various values of the reduced strength parameter L. This graph is to be used for the convergent plane of a quadrupole with real object and real image. Distances are measured from the effective ends of the quadrupole. $P' = p'/l$, $Q' = q'/l$, $L = kl$.
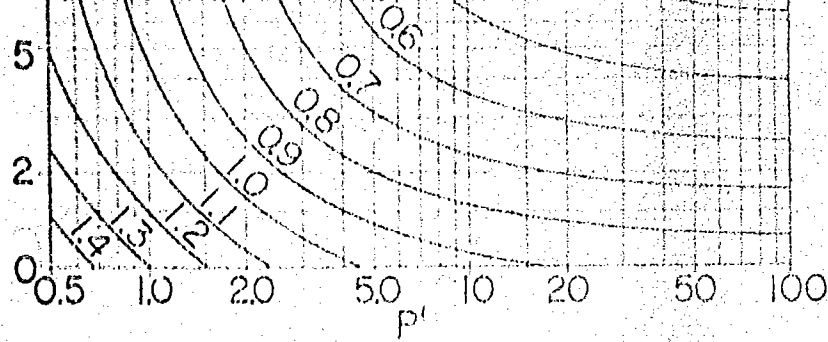
FIG. 9. Graphical presentation of quadrupole optics. The reduced image distance Q' and magnification m are given as functions of reduced object distance P' for various values of the reduced strength parameter L. This graph is to be used for the convergent plane of a quadruple with real object and real image. Distances are measured from the effective ends of the quadrupole. $P' = p'/l$, $Q' = q'/l$, $L = kl$.
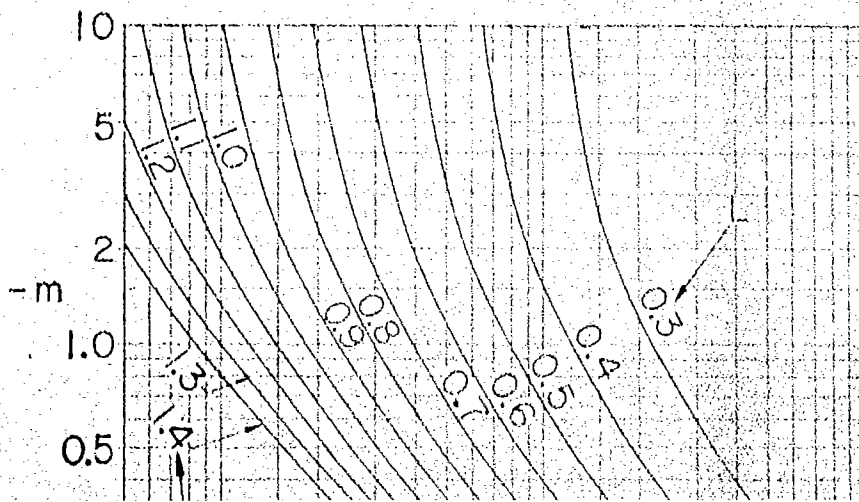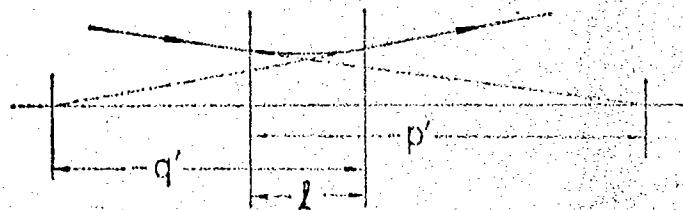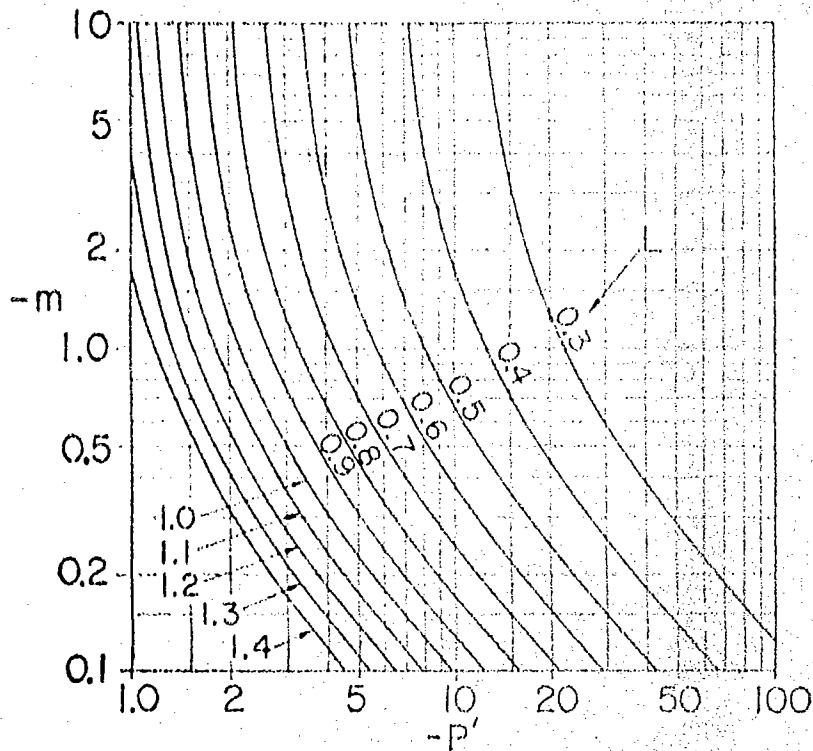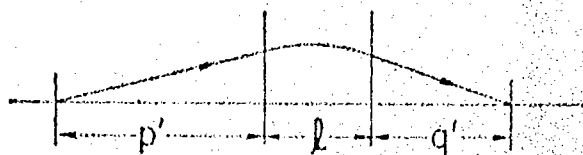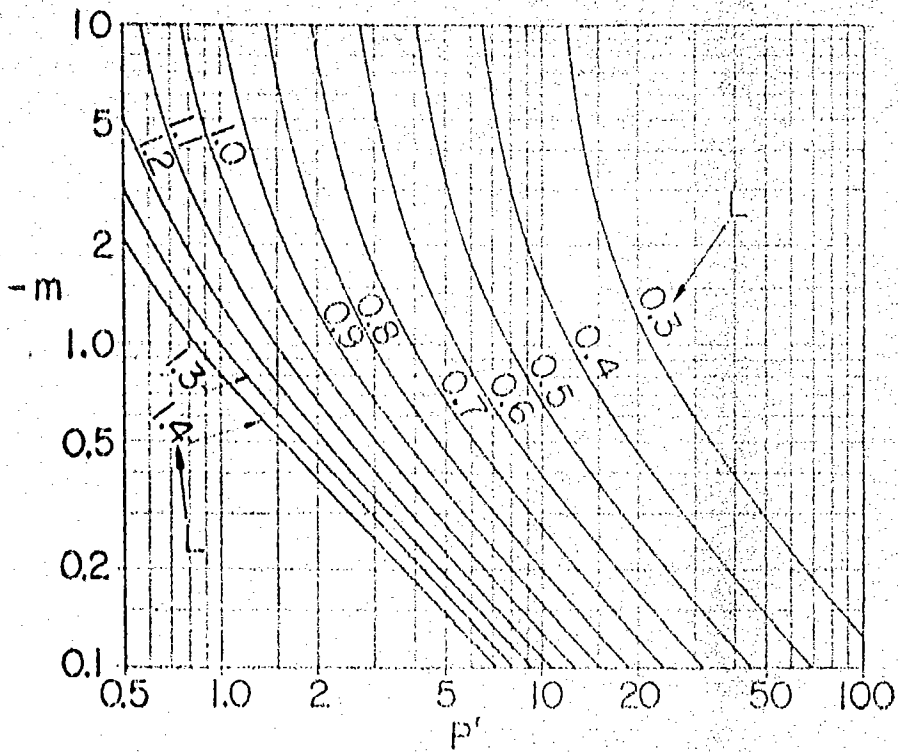
FIG. 10. Graphical presentation of Q' and m for various P' and L; Divergent plane of quadrupole, virtual object, and virtual image. Notice negative P' implies a virtual object and Q' has a similar implication.
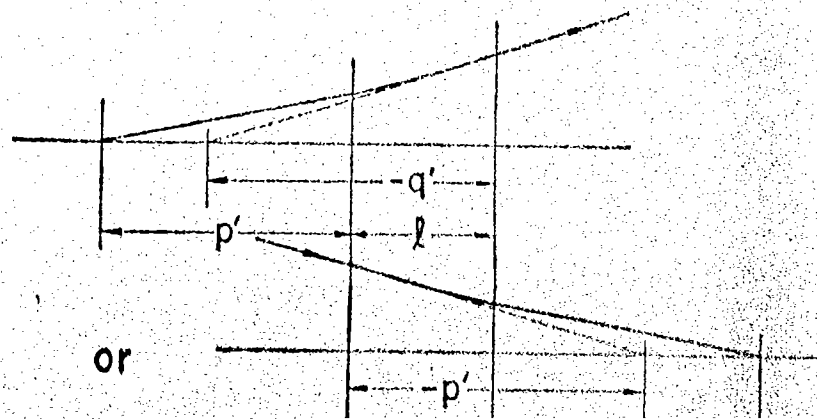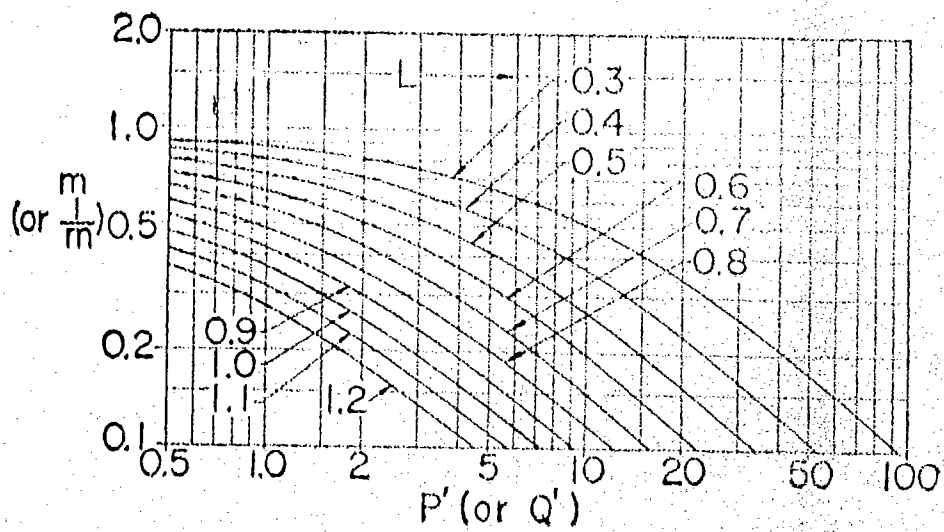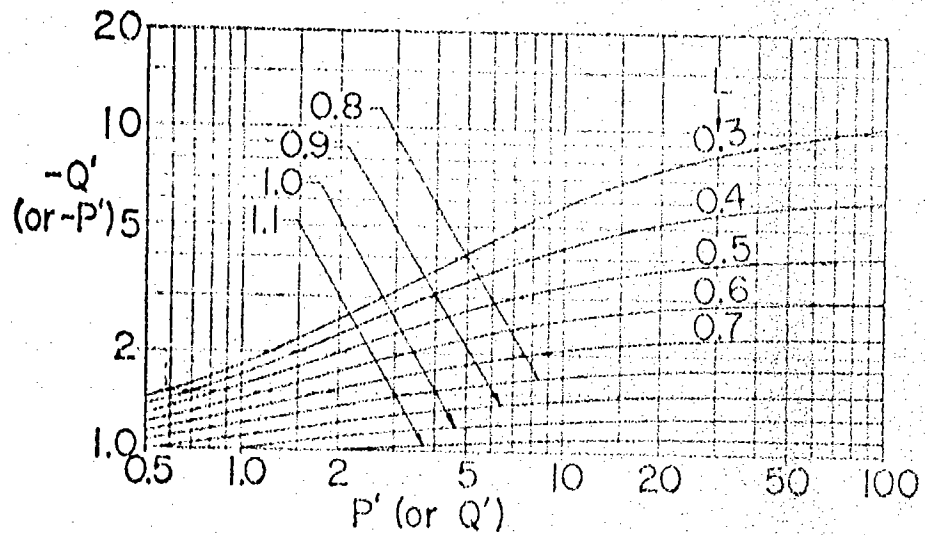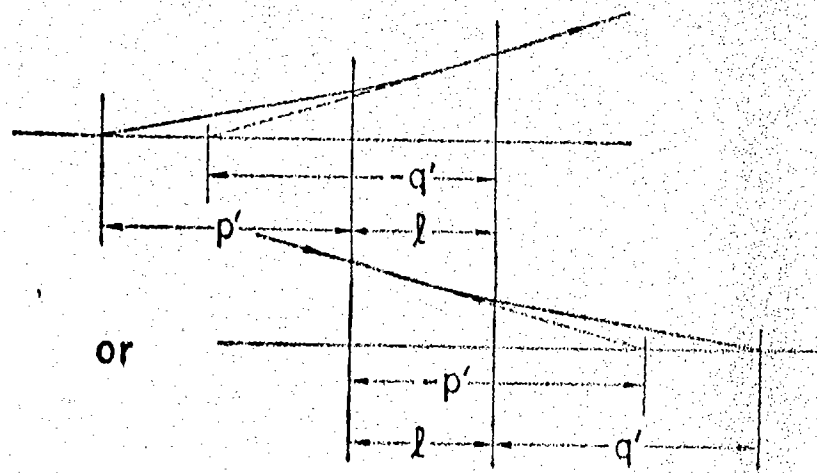
FIG. 11. Graphical presentation of Q' and m for various P' and L: divergent plane of quadrupole, real object, and virtual image, or virtual object and real image. We use the relations $P' = p'/l$, $Q' = q'/l$, $L = kl$.

(a)

(b)

FIG. 12. Quadrupole lenses. (a) Doublet lens. (b) Triplet lens.
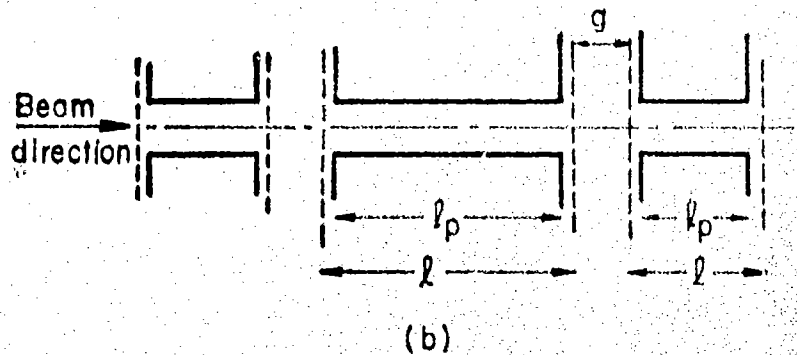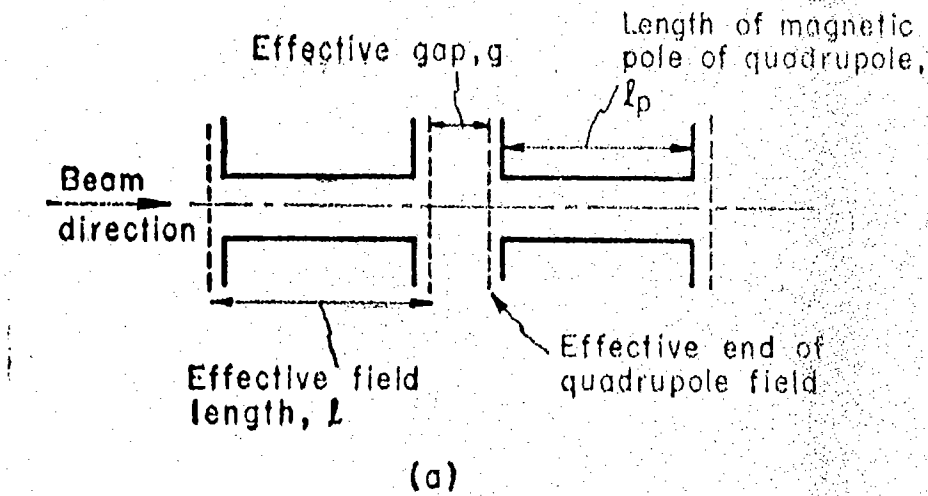
FIG. 12. Quadrupole lenses. (a) Doublet lens. (b) Triplet lens.
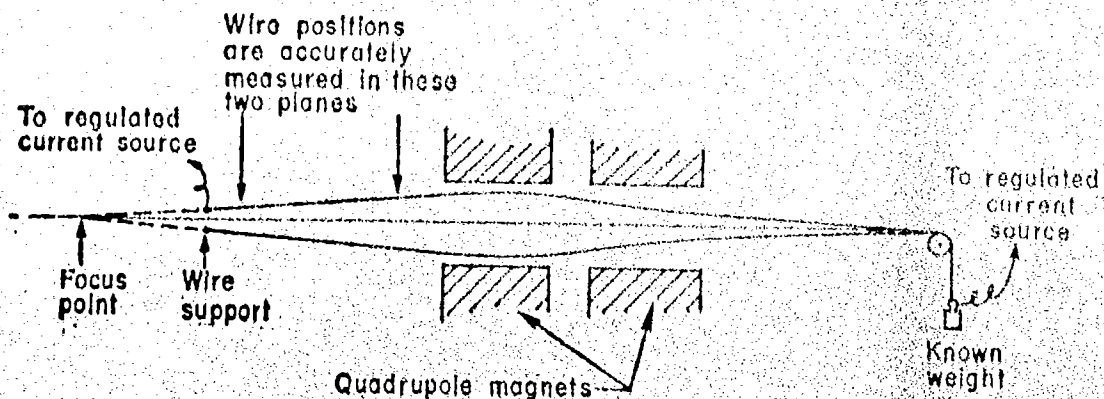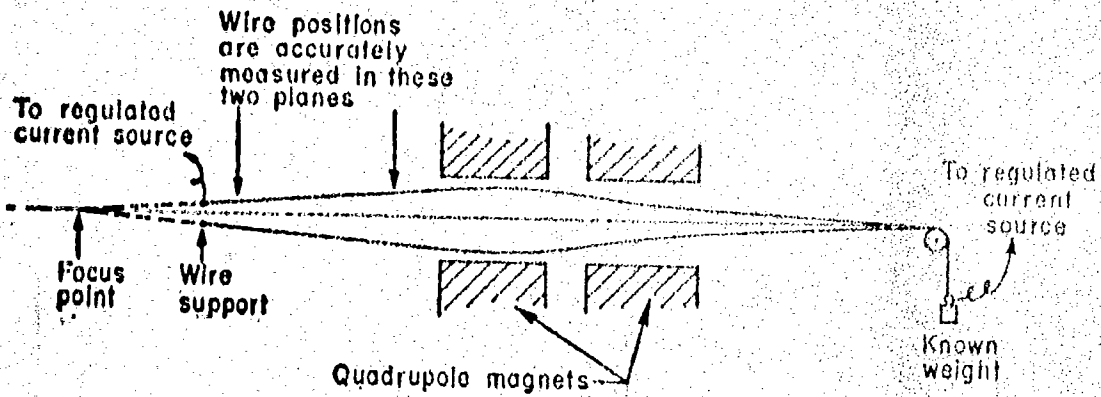
FIG. 13. Arrangements for measuring focal properties of a pair of quadruples.
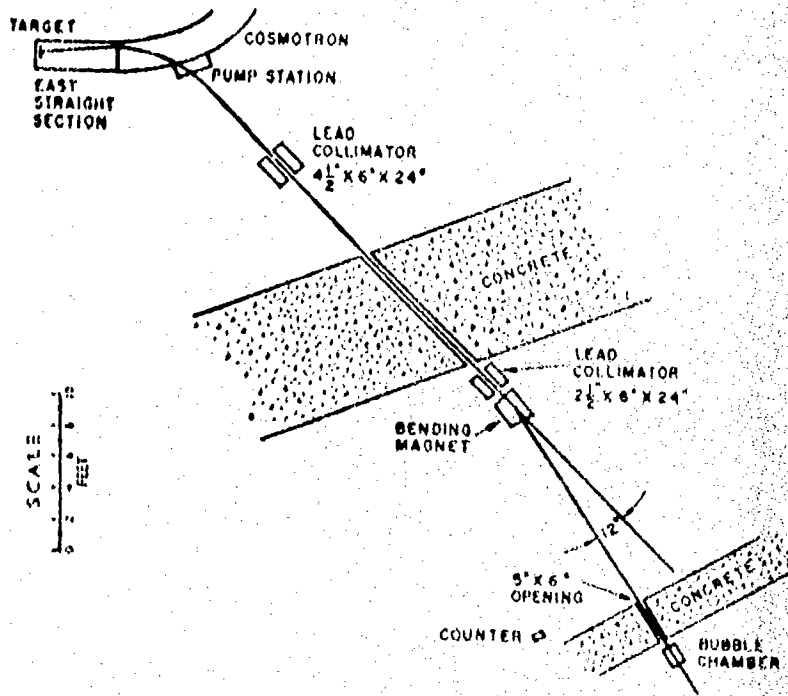
FIG. 14. Experimental apparatus of Chretien, Leitner, Samios, Schwartz & Steinberger for providing a π^- beam at 1.4 Bev/c.
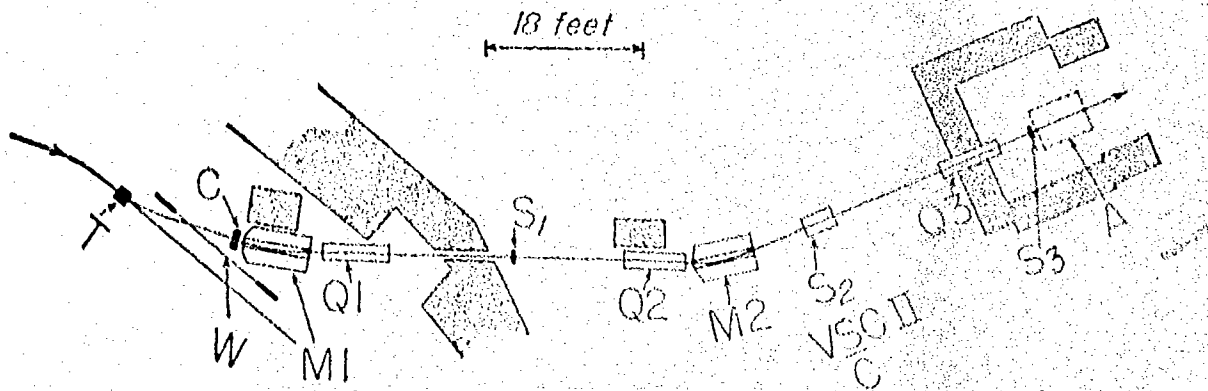
FIG. 15. Double spectrograph used for antiproton experiments by Elioff, Agnew, Chamberlain, Steiner, Wiegand & Ypsilantis. Deflecting magnets are indicated as $M1$ and $M2$. Triplet quadrupole lenses are $Q1$, $Q2$, and $Q3$. The initial bending of the orbit near the target T is due to the field of the Bevatron.
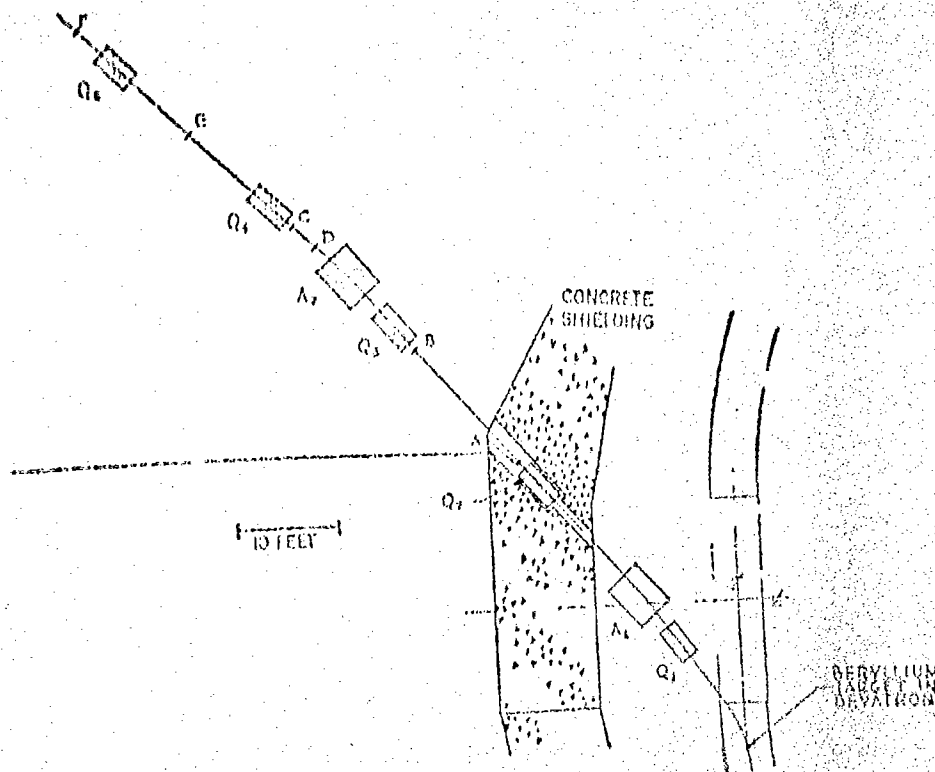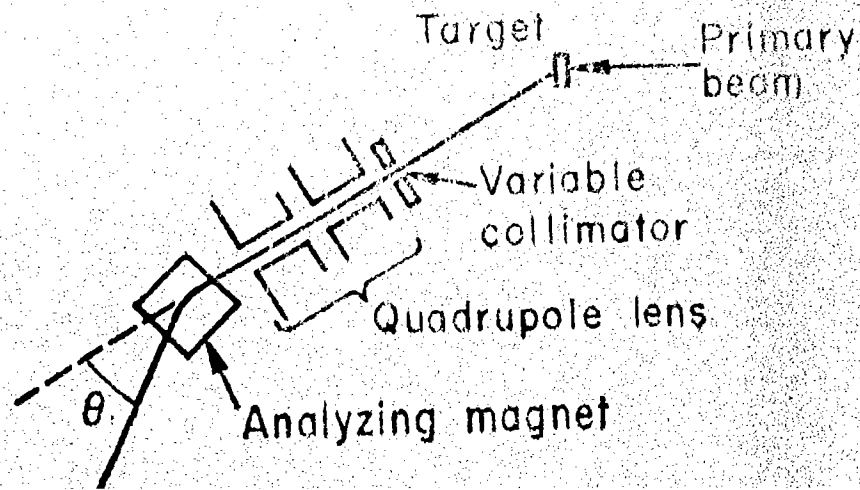
FIG. 16. Arrangement of Cork, Lambertson, Piccioni & Wenzel for antiproton experiments. The second and fourth quadrupole lenses Q_2 and Q_4 act as field lenses. The quadrupole system, if used without the deflecting magnets A_1 and A_2, could pass a wide band of momenta.
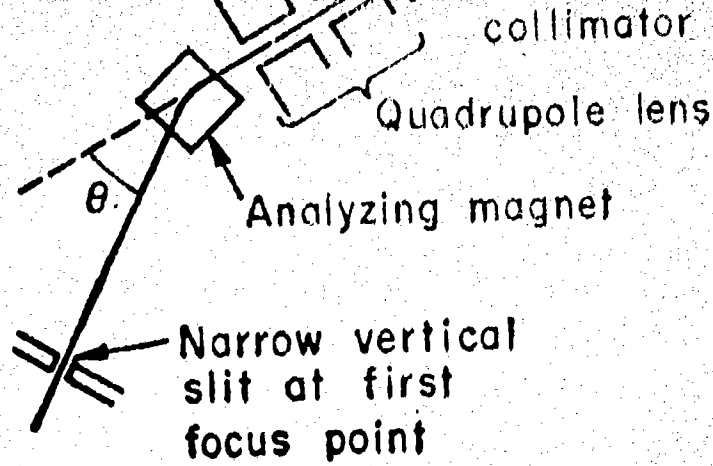
collimator

Quadrupole lens

θ

Analyzing magnet

Narrow vertical
slit at first
focus point

Fig. 17. Insertion of a variable collimator and narrow vertical slit for the determination of beam intensity under conditions of known acceptance A. A necessary condition is that the observed beam intensity be proportional to collimator area and to slit width.
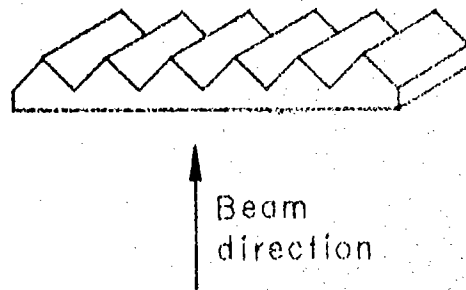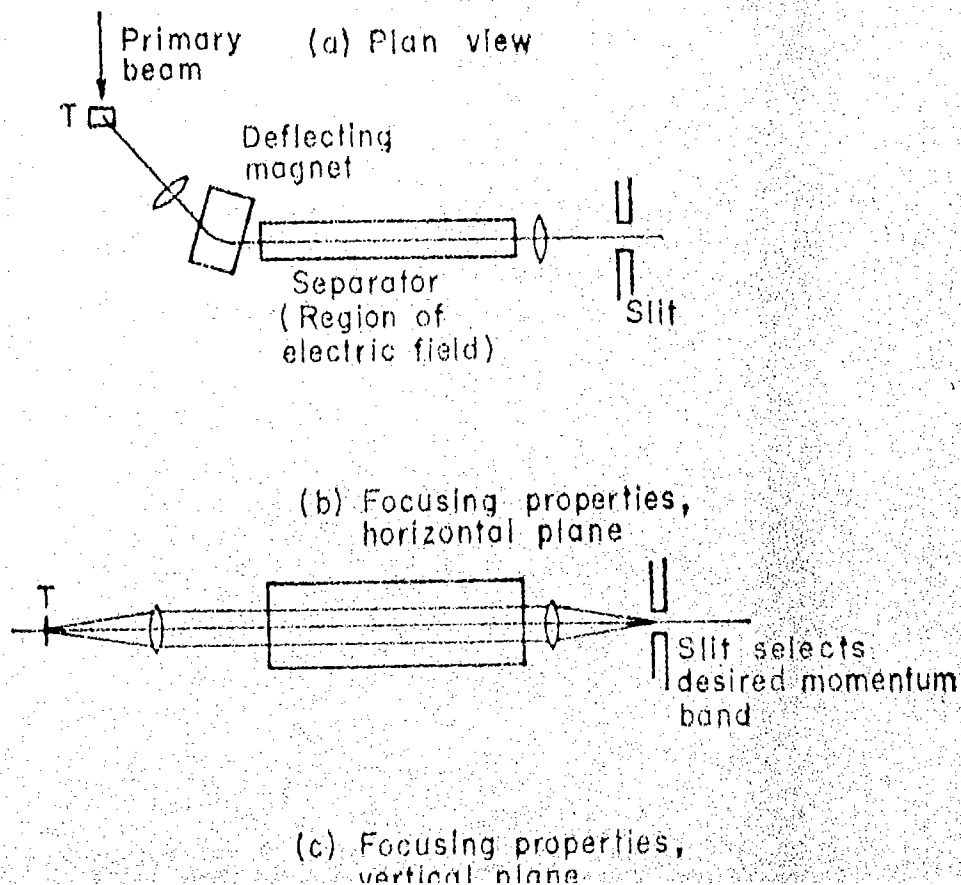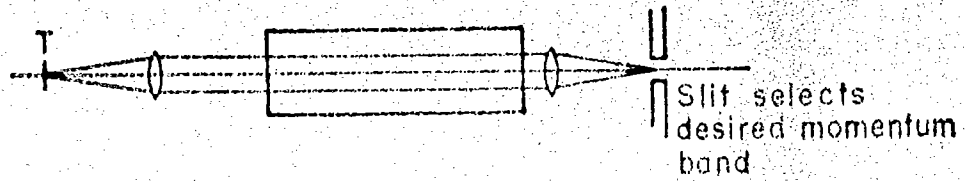
Beam
direction

Fig. 18. Ribbed absorber for converting a monoenergetic beam into a "white" beam suitable for evaluating the acceptance of a magnet system.

Primary   (a) Plan view
beam

T

Deflecting
magnet

Separator
(Region of
electric field)

Slit

(b) Focusing properties,
horizontal plane

T

Slit selects
desired momentum
band

(c) Focusing properties,
vertical plane

(b) Focusing properties, horizontal plane

Slit selects desired momentum band

(c) Focusing properties, vertical plane

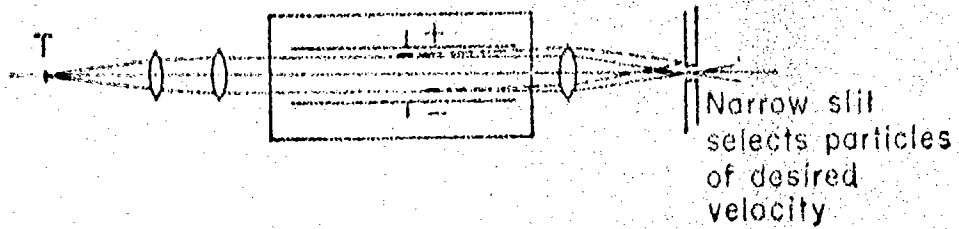Narrow slit selects particles of desired velocity

Fig. 19. Schematic presentation of a one-stage separated-beam apparatus with parallel-plate separator.